Australian Tornadoes in 2013: Implications for Climatology and Forecasting

JOHN T. ALLEN,^a EDWINA R. ALLEN,^b HARALD RICHTER,^c AND CHIARA LEPORE^d

^a Department of Earth and Atmospheric Sciences, Central Michigan University, Mt. Pleasant, Michigan
 ^b Department of Biology, Central Michigan University, Mt. Pleasant, Michigan
 ^c Bureau of Meteorology, Melbourne, Victoria, Australia
 ^d Lamont Doherty Earth Observatory, Columbia University, New York, New York

(Manuscript received 29 July 2020, in final form 17 January 2021)

ABSTRACT: During 2013, multiple tornadoes occurred across Australia, leading to 147 injuries and considerable damage. This prompted speculation as to the frequency of these events in Australia, and whether 2013 constituted a record year. Leveraging media reports, public accounts, and the Bureau of Meteorology observational record, 69 tornadoes were identified for the year in comparison to the official count of 37 events. This identified set and the existing historical record were used to establish that, in terms of spatial distribution, 2013 was not abnormal relative to the existing climatology, but numerically exceeded any year in the bureau's record. Evaluation of the environments in which these tornadoes formed illustrated that these conditions included tornado environments found elsewhere globally, but generally had a stronger dependence on shear magnitude than direction, and lower lifting condensation levels. Relative to local environment climatology, 2013 was also not anomalous. These results illustrate a range of tornadoes associated with cool season, tropical cyclone, east coast low, supercell tornado, and low shear/storm merger environments. Using this baseline, the spatial climatology from 1980 to 2019 as derived from the nonconditional frequency of favorable significant tornado parameter environments for the year is used to highlight that observations are likely an underestimation. Applying the results, discussion is made of the need to expand observing practices, climatology, forecasting guidelines for operational prediction, and improve the warning system. This highlights a need to ensure that the general public is appropriately informed of the tornado hazard in Australia, and provide them with the understanding to respond accordingly.

KEYWORDS: Severe storms; Storm environments; Tornadoes; Climatology; Convective storms; Mesoscale forecasting

1. Introduction

In 2013, Australia experienced a supposed record tornado season, especially when compared to historical context. However, nearly 25 years after the publication of Geerts and Noke-Raico (1995), the scientific community is still little the wiser as to the actual frequency of tornadoes in Australia, or the conditions favorable for their occurrence. Tornadoes in Australia have been described since the first recorded event in Sydney in 1795. However, despite every year since 1850 having at least one documented tornado observation according to the Bureau of Meteorology (BoM) Severe Thunderstorm Archive [STA; BOM (2020) and Allen and Allen (2016)], it is unclear how many of these events occur annually.

Early Australian tornado investigations focused on case studies of events that drew commonality with tornadoes observed in the United States. Later studies continued to apply this association, (e.g., Clarke 1962; Evesson 1970; Minor et al. 1980; Allen 1980), though intensity and frequency appeared to be less for Australia (Fujita 1973; Grazulis 1993). Owing to the relatively sparse observations, much of the country was identified to have a low tornadic frequency. However, the coastal areas of New South Wales did appear to have a frequency comparable to parts of the northern U.S. Great Plains. In contrast, the highest formal rating in the STA applied to a tornado in Australia is F3 (Fujita 1971), though several

Corresponding author: John T. Allen, johnterrallen@gmail.com

unsurveyed events may have produced far stronger winds over underpopulated areas (Minor et al. 1980; Geerts and Noke-Raico 1995). This suggests that violent tornadoes are possible, but likely rare events. As the focus here is on characterizing tornadoes in 2013, we refer the reader to a more comprehensive review of tornadoes in Australia (Allen and Allen 2016), which discusses both existing climatology and case studies. Recent studies have also examined high-impact cases over southeast Queensland, the south coast of New South Wales, and Tasmania (Louis 2018; Fox-Hughes et al. 2018; Soderholm et al. 2020b). However, as recently as 2002, only 700 tornadoes existed in the STA database, suggesting that 2013 may be unusual. Given that the STA database only includes 1293 tornadoes in 220 years (1795–2014), this suggests that placing the tornadoes for Australia in 2013 into context may be difficult, and not reflective of the true climatological frequency.

To add context, atmospheric regimes and environments favorable for tornadoes can be considered based on those established globally. These environments can be used to identify the potential where observations are lacking, and indicate predictability. Common to all the formative environments is the presence of high near-surface helicity or vertical wind shear (hereafter shear) to introduce storm rotation, and relatively low cloud bases (Brooks et al. 2003; Thompson et al. 2003; Grams et al. 2012; Garner 2013). Instability is also a requisite ingredient for the presence of a thunderstorm, however instability for tornado formation can range considerably, with convective available potential energy (CAPE) from $100\,\mathrm{J\,kg^{-1}}$ to as much as $9000\,\mathrm{J\,kg^{-1}}$ (Hanstrum et al. 2002;

Rasmussen 2003; Edwards 2012; Sherburn et al. 2016). Tornado formative environments can range from those balancing shear and instability (Johns et al. 1993; Rasmussen 2003; Grams et al. 2012; Coffer et al. 2019), to instability rich environments compensating via boundary-induced helicity or changes in wind direction (e.g., Garner 2013; Boustead et al. 2013). At the other end of the spectrum there are also low-level shear driven environments with limited instability that can arise in winter associated with intensely cold upper air (e.g., Hanstrum et al. 2002; Mills 2004; Richter 2007; Kounkou et al. 2009; Sherburn et al. 2016) or in the outer bands of tropical cyclones where low-level instability can combine with strong low-level shear (e.g., McCaul 1991; Edwards 2012; Onderlinde and Fuelberg 2014; Jones et al. 2019). The most heavily studied are the springtime moderate to high shear and high buoyancy environments of the central United States (e.g., Grams et al. 2012), however, globally such moisture-rich environmental conditions are rare. Our principle interest is not to illustrate that there are many different "types" of environments producing tornadoes, as many events produce significant damage (Grams et al. 2012; Coffer et al. 2019), but rather highlight that tornadoes can occur in a wide set of environmental conditions, and that these conditions can and have occurred in Australia. Environmental characterization for tornadoes has been made easier using atmospheric reanalysis products (Brooks et al. 2003; Brooks 2009; Allen and Karoly 2014), which provide long temporal records of atmospheric variables. For example, Brooks et al. (2003) showed that few Australian cases met the U.S. derived thresholds for tornadic environments. However, the NCEP-NCAR reanalysis had relatively coarse resolution (2.5°), hence there was potential for underestimation as compared to recent high-resolution reanalyses (e.g., Gelaro et al. 2017). More recent studies have suggested that environments favorable to the development of organized and severe convection are not infrequent, particularly over the eastern half of Australia (Allen et al. 2011; Allen and Karoly 2014). This suggests sufficient potential to support the development of storms that produce tornadoes at least occasionally.

No large sample of tornadoes has been available to develop understanding of tornadically favorable environments over Australia, which has implications for the forecasting process. Existing forecast guidelines in Australia primarily rely on the use of the National Thunderstorm Forecast Guidance System [NTFGS; Mills and Colquhoun (1998) and Deslandes et al. (2008)]. These use decision-tree thresholds to indicate whether conditions are likely to produce convective hazards such as tornadoes, large hail, or damaging winds. A significant limitation of NTFGS is that it is a dichotomous or trichotomous prediction algorithm and is not probabilistically continuous, and is uncalibrated or based on small sample sizes. The decision for tornadoes relies on satisfying the threshold criteria based on a small sample of storms (G. Mills 2016, personal communication), neglecting cases in locally modified environments (e.g., tropical cyclones, near mesoscale boundaries, or atypical environments). The tornado thresholds also involve a two-step decision: whether an environment is favorable to cool season (Hanstrum et al. 2002; Mills 2004) or warm season tornadoes, with the subsequent thresholds based on both shear and a lifted index. Given the small body of available literature and case studies of tornadoes in Australia (Allen and Allen 2016), this suggests motivation to improve tornado forecasting parameters for Australian conditions.

The motivation behind this exploratory study is whether the frequency of Australian tornadoes during the year 2013 was exceptional relative to climatology. Arising from this question, we explore whether the environmental conditions associated with these Australian tornadoes are common to other parts of the world, and whether existing parameters can improve our understanding of climatology and predictability. Finally, the steps toward improving documentation of tornado events are discussed, and whether the risk indicates a need for updating forecasting and warning approaches.

2. Data and approach

a. Observations

To provide the reference climatology, BoM STA historical tornado reports were collected for the period 1795–2014 (BOM 2020). Quality control for these data are limited, and metadata rarely includes rated tornado strength or other characteristics. To avoid these problems, we extract latitude, longitude, date, and time information, which are available in all cases and use this information to produce a comparative climatology. Data are gridded to an $80 \, \mathrm{km} \times 80 \, \mathrm{km}$ grid, following the approach of Allen and Allen (2016).

To identify tornado events or confirm official STA records for 2013 (BOM 2020), evidence was gathered via search terms via Google for storm damage, and subsequent metasearching to identify eyewitness accounts and imagery describing the nature of the event (see appendix for further details). This approach identified cases in newspapers and news outlets, YouTube, weather and outdoor forums, and social media. Events were labeled as definite, likely, or unconfirmed, with nearly all events associated with sufficient evidence to confirm the likely or definite presence of a tornado based on the criteria of Evesson (1970) and Allen (1980), and each case was crossvalidated using radar information (Table A1). Where possible, path characteristics were determined using a combination of evidence sources, radar, and Google Earth satellite imagery. Path width and length were difficult to determine for most events where there was no official effort to survey damage paths, but were ascertained by use of street view and known locations in Google Earth. Based on all visual and descriptive evidence tornadoes were then rated into one of three categorizations: weak (encompassing F0-F1), strong (F2-F3), and violent (F4–F5), with the estimated F-scale indicated. This approach is not without limitations, as this can lead to the potential for over or underrating of tornado intensity, as sources might not include the greatest damage, or alternatively focus on the most significant damage. The choice to use the Fujita scale with modifications for structural differences (Fujita 1971), as opposed to the enhanced Fujita scale (Doswell et al. 2009) reflects the lack of common damage indicators between North America and Australia (Sills et al. 2004; Edwards et al. 2013).

To evaluate tornadoes during 2013 associated with tropical cyclones, historical track position data for tropical cyclones

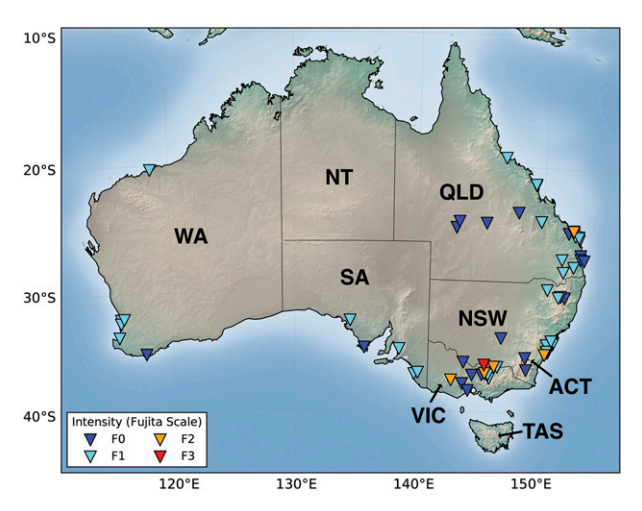


FIG. 1. Map of the latitude and longitude locations of the 69 Australian tornadoes that occurred in 2013, delimited by estimated Fujita scale rating. States are indicated by their respective boundaries and common abbreviations: Queensland (QLD), New South Wales (NSW), Victoria (VIC), Tasmania (TAS), South Australia (SA), Western Australia (WA), Northern Territory (NT), and Australian Capital Territory (ACT).

were obtained from the IBTrACS dataset (Knapp et al. 2010), and archived BoM operational forecasts for tropical low segments.

b. Reanalysis

To analyze the environmental conditions we apply the Modern-Era Retrospective Analysis for Research and Applications, version 2 (MERRA2), dataset (Gelaro et al. 2017). MERRA2 is a $0.5^{\circ} \times 0.625^{\circ}$ reanalysis product developed by NASA with 72 model levels at 3-hourly temporal resolution for the period 1980–2019 focusing on incorporation of satellite observations in addition to common reanalysis observations. Vertical profiles were evaluated for convective parameters over the Australian domain (Fig. 1) using a newly developed Python package, from pressure (P), temperature (T), specific humidity (Q), zonal and meridional winds (U and V) on model levels appended to the surface pressure, and 2 m (T, Q) and 10 m (U, V) analysis fields at each grid point. Derivative parameters were calculated (e.g., dewpoint) and above ground level (AGL) layer height was determined by solving the hypsometric equation. CAPE was calculated for a variety of parcels, including for the 50 and 100 hPa mixed-layer (ML), most unstable (MU), and surfacebased parcels (SB). Lifting condensation levels were calculated using the Stull approximation (Stull 2000). Storm relative helicity was calculated for the 0-1 km (SRH1) and 0-3 km (SRH3) layers using storm motions inferred from the Bunkers technique using the mean 0-6 km unweighted wind velocities and applying both the left- and right-moving storm propagation (Bunkers et al. 2000). Bulk vertical wind shears were calculated by vertical interpolation of U and V to the appropriate AGL reference heights (0–1 km; S01 and 0–6 km; S06), while lapse rates were similarly obtained (0-3 km lapse rate, 700-500 hPa lapse rate). Composite parameters, including the significant tornado parameter (STP) and supercell composite parameter (SCP), were also computed using the standard (fixed-layer) approach of Thompson et al. (2003) for both left-and right-moving storms.

Proximal case soundings from the reanalysis were determined using a radial search of the nearest land grid point (landsea mask ≥0.3) and the eight surrounding grid points (±1 latitude–longitude grid), selecting the grid point with the most unstable 50 hPa MLCAPE, and temporal proximity fixed to the nearest prestorm MERRA-2 time step (equivalent to within 3 h of the event), similar to the criteria proposed by Potvin et al. (2010). Each tornado event was classified according to the prevailing synoptic and thermodynamic conditions as cool or warm season using the NTFGS criteria (Mills and Colquhoun 1998), which specifies a threshold of below or above 12°C at 850 hPa, and then checked to assess whether a storm was within the cloud structure or 250 km of a large-scale environment produced by an active tropical cyclone (TC) or an east coast low (ECL).

c. Radar classification

Classification was also made for all 2013 tornadoes where radar data were available (Table A1) to classify storm mode in order to better understand underlying environments. Storms were subjectively classified by mode using the nearest proximal radar from the Australian radar network (The Weather Chaser 2017) using reflectivity and, where available, Doppler velocity. Where no velocity information was available, storm longevity, and storm motion deviant relative to the mean flow was used to assess storm organization. The categories were assigned as supercellular, whether rotation could be inferred as left moving or right moving, or disorganized.

3. Review of 2013 tornadoes and associated environments

a. Overview

A total of 69 tornadoes occurred in Australia during 2013, with at least 1 tornado in every state and territory except TAS and NT (Table 1, Fig. 1). No significant tornadoes impacted the major cities; however, the human impact was anomalous, with 147 reported injuries and no fatalities for 2013 (Table A1), compared with 116 injuries and 28 fatalities for the remainder of the 1795-2014 STA record. However, the STA record does not always include injury information (e.g., it contained no injuries or fatalities for 2013), and media reports document greater numbers of injuries for historical events (Allen and Allen 2016). Spatially, the tornadoes that occurred during 2013 reflect the distribution expected from the population distribution (Fig. 2a), with a greater frequency where density is higher. In comparison to the gridded tornado reports in the existing STA record, only three tornadoes from 2013 occurred outside of a grid box with at least one recorded tornado for the period 1795-2014, though even these three occurred in a neighboring grid box to recorded tornadoes (Fig. 2b). The spatial frequency inferred from the STA also likely underestimates the risk, given that only 100 tornadoes are documented before 1900. Nonetheless, this suggests that 2013 does not

TABLE 1. Summary of 2013 tornadoes by Australian state. Rating is split into weak (F0–F1) or strong (F2–F3), and the season in which tornadoes occurred determined based on the 850 hPa temperatures exceeding or below 12°C as warm season (WS) or cool season (CS). This classification was only applied in cases where a tornado was not associated with a tropical cyclone (TC) or east coast low (ECL). Storm mode was broken down for WS and CS cases into either tornadoes associated with a radar-determined supercell (Supercell) or disorganized (Disorg.) including quasi-linear convective systems and nonsupercellular cases.

State	Tornadoes	Weak	Strong	WS	CS	TC	ECL	Supercell	Disorg.
QLD	24	23	1	11	0	13	0	8	3
NSW	17	16	1	3	3	0	10	6	0
VIC	15	11	4	8	7	0	0	10	5
WA	7	7	0	3	4	0	0	7	0
SA	5	5	0	1	4	0	0	4	1
ACT	1	1	0	1	0	0	0	1	0
All	69	91.3%	8.7%	39.1%	26.1%	18.8%	14.5%	49.3%	13.0%

appear exceptional or unprecedented in terms of the observed spatial distribution.

A total of 31 days in 2013 produced 1 or more tornadoes (Table A1); 12 days produced 2 or more tornadoes. During the calendar year, no tornadoes were rated in the STA as violent. However, this is unsurprising given that the STA includes no surveyed verifiable violent tornadoes for 1795–2014, partly contributed to by only 19% of observations including rating data. This contrasts with more recent efforts to expand this database, which remain ongoing (Allen and Allen 2016), that indicate such events may be more frequent than currently implied, with some known violent events not officially surveyed. Nonetheless, strong tornadoes made up a substantial fraction of the events for this year (6 tornadoes F2+, or 9.1%). Four days met the definition for a tornado outbreak of 6 or more tornadoes (Tippett et al. 2016).

January was an active month for tornadoes, with 21 (Fig. 3a), primarily due to an outbreak of 13 tornadoes from 23 to

27 January 2013 with the east coast passage of ex-Tropical Cyclone Oswald. Other events in January included several tornadoes with discrete supercells in QLD, WA, NSW, and VIC. February was also relatively active, with moderate damage arising from eight tornadoes associated with an ECL over coastal NSW. March also had an outbreak event in northern VIC, before cool season tornado days became more prevalent from April to September, which included generally isolated events in WA, SA, QLD, and VIC. Through spring (September-November), frequency increased, especially into November, with an outbreak in northeastern NSW. Comparing the number of 2013 tornado reports to the historical number of reports per calendar day (Fig. 3a), the tornado outbreaks produced frequencies substantively above STA climatology.

Diurnally in 2013, tornado frequency fraction is shifted toward the late afternoon hours compared to historical climatology (Fig. 3b). This analysis, however, does not exclude the default reports in the STA dataset from 0000 to 1400 UTC

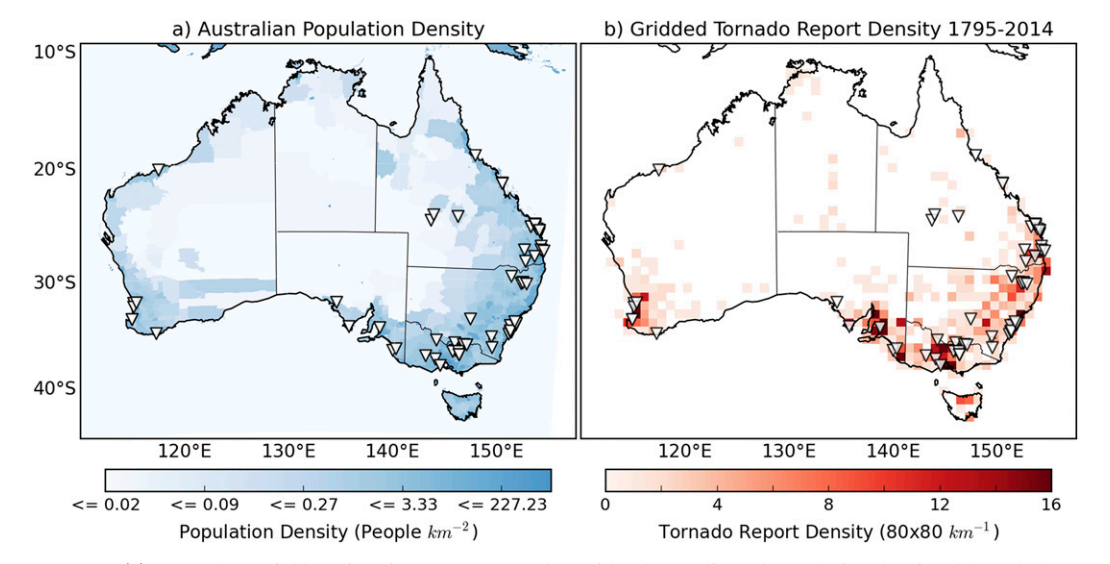


FIG. 2. (a) Tornado spatial locations in 2013 compared to gridded nonadjusted population density chloropleth as of the year 2000 from the Center for International Earth Science Information Network Gridded Population of the World, version 3, at 2.5 arc-min resolution. (b) Total density of BoM STA-sourced tornado reports from 1795 to 2014, aggregated on a $80 \, \text{km} \times 80 \, \text{km}$ grid and overlaid with point reports from 2013.

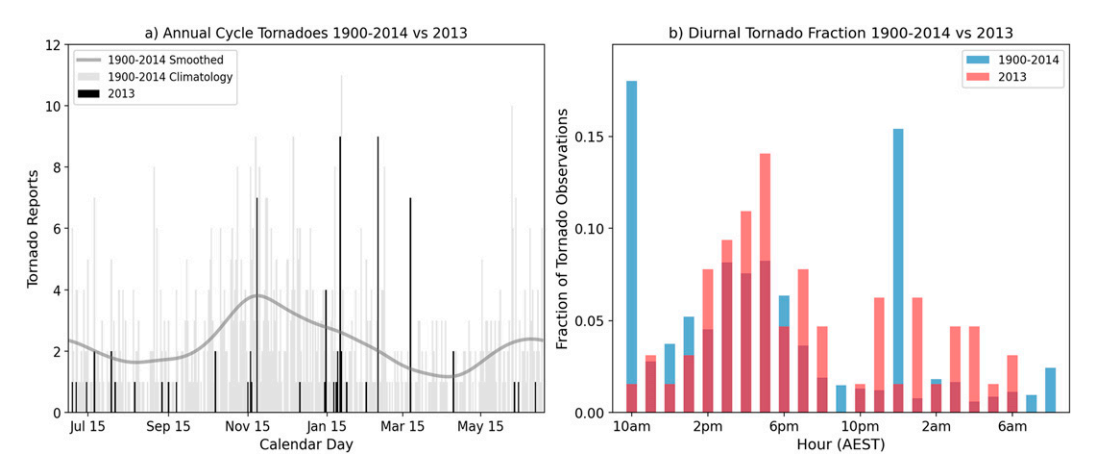


FIG. 3. 2013 Australian tornado events in the context of the annual and diurnal cycles determined from the 1161 Bureau of Meteorology STA tornado reports for the period 1900–2014. (a) Annual cycle fitted with a periodic 15-day Gaussian kernel smoothing procedure to preserve the structure of the cycle at the end-of-year boundaries, with the *x* axis centered to illustrate the peak of the austral summer. Gray lines show the underlying daily histogram of daily tornado reports, while the black lines reflect tornadoes on each calendar day in 2013. (b) Hourly proportions of tornadoes within a full diurnal cycle in AEST for the 1161 1900–2014 STA tornadoes (blue) and the 2013 tornado observations (red). Overlapping columns (burgundy) indicate where the fractions overlap. Where blue columns are larger, there is a larger fraction of STA tornado reports, while red columns indicate that the 2013 reports have a larger fraction at a given hour. Display is chosen such that the axis begins at 1000 AEST (0000 UTC).

(from 1000 to 0000 AEST), where time information was either unknown or incorrectly entered, and thus may not represent climatology (T. Wedd 2020, personal communication). The relative fraction of reports in the early hours of the morning during 2013 is somewhat unusual, particularly associated with the ECL, reflecting a period where fewer tornado reports are typically recorded anywhere in the world (Ashley et al. 2008). This also highlights a source of risk owing to the difficulty in warning populations during overnight hours.

Five case studies exemplary of multiple tornado report events in Australia were next explored in terms of their formative environment and synoptic setting.

b. Ex-Tropical Cyclone Oswald

Landfalling tropical cyclones are well known to produce tornadoes (Verbout et al. 2007; Edwards 2012). From 23 to 27 January 2013, an ex-tropical cyclone made landfall on the QLD coast between Mackay and Tweed Heads. The storm moved southward along the coastline, producing heavy rainfall, strong winds and at least thirteen tornadoes (Fig. 4a). The majority of these tornadoes began over the water before producing damage over the coastal fringe. Damage from these tornadoes was relatively minimal, and flooding precluded formal survey of the damage paths. Analysis of damage photographs and video suggests that none of these tornadoes exceeded F2 strength. On 25 January at Hay Point a tornado impacted the local automatic weather station. Peak wind speed recorded was 139 km h⁻¹ at 0415 local time (LT), accompanied by reports of minor damage and an observed hook echo on Doppler radar. Wind observations before and after the tornado's passage were 5 and $7 \,\mathrm{km}\,\mathrm{h}^{-1}$. As the cyclone moved southward along the coast, several tornadoes occurred on 26 January with the strongest near Bargara (Fig. 4a; tornado 3). The Wide Bay region would experience a further seven tornadoes in the following 12 h, including two striking Burnett Heads (tornadoes 4 and 7) and one at Coonarr (tornado 5).

The tornadoes that accompanied Oswald were each associated with a significant low-level mesocyclonic signature on Doppler radar, with these storms occurring in the region where the onshore low-level jet of the system was preferentially stronger. This led to a region of extremely favorable long cyclonic hodographs, particularly in the lowest 3 km (Fig. 4d). The cells moved onshore from a north-northeasterly direction, with the signatures dissipating shortly after landfall in each case. The area of maximized SRH1 corresponds to a region where low level winds backed to the east 4c). SRH3 values inland were as high as $-320 \,\mathrm{m}^2 \,\mathrm{s}^{-2}$, while the majority of tornadoes occurred in a region characterized by 18 m s⁻¹ of S06, and -160 to -200 m² s⁻² SRH1. Typical of tropical cyclone environments, this led to a region of strong low-level shear intersecting low MLLCLs associated with the near-saturated moist onshore airflow (Fig. 4c). The final component leading to the outbreak was the development of moderate instability with CAPE of generally 600–1200 J kg⁻¹. Enhancing the potential for tornadoes was low-level instability as reflected by the 0-3 km lapse rates near 6 K km⁻¹ (Fig. 4c). This combination of factors led to STP less than -1, reflecting potential for significant tornadoes confined to the near-coastal plain and hills around Bundaberg. Higher-resolution model data has highlighted the importance of locally enhanced helicity in the formation of the tornadoes on the day and yielded even higher SRH1 (Ramsay et al. 2013).

Summarizing this case, the presence of strong low-level shear across a surface boundary, appreciable midlevel lapse

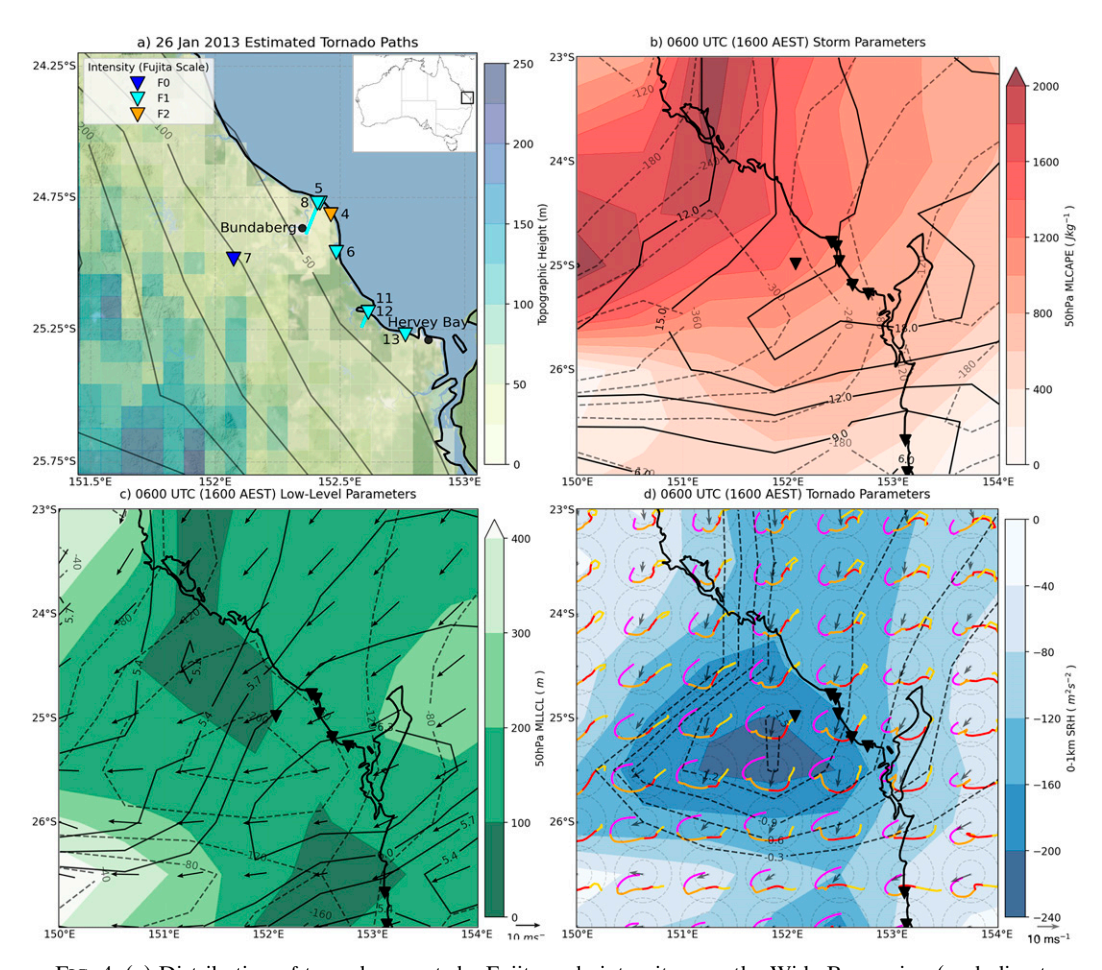


FIG. 4. (a) Distribution of tornado reports by Fujita scale intensity over the Wide Bay region (excluding tornadoes 1–3, 9, and 10, which occur outside this domain) during ex–Tropical Cyclone Oswald for 26 Jan 2013, with region relative to Australia inset, and topography from gridded NOAA/NGDC ETOPO5 5 min × 5 min data, and MERRA-2 contoured topography. (b) MERRA-2 derived storm parameters including 50 hPa mixed-layer CAPE (MLCAPE) at 0600 UTC, with 0–6 km bulk vertical wind shear (S06; black contours), and 0–3 km storm-relative helicity (SRH3; gray dashed). (c) 50 hPa mixed-layer LCL (MLLCL) with 0–3 km temperature lapse rates (black contours), 0–1 km storm-relative helicity calculated assuming the left mover as calculated from the internal dynamics method (SRH1; gray dashes), and 50 m wind vectors. (d) SRH1 contours illustrating the strong axis of enhanced near-surface helicity over the region (blue filled contours), with significant tornado parameter for the left mover (STP; dashed contours). Scaled storm-relative hodographs are shown for each grid point, with Bunkers et al. (2000) internal dynamics estimates of left-mover storm motion shown by the arrows. Hodograph range rings indicate velocities of 7.5 and 15 m s⁻¹, respectively. Hodograph color corresponds to ground-relative height: 0–1 (magenta), 1–3 (orange), 3–6 (red), and 6–9 km (yellow). Each panel shows the location of the tornado reports in the region from (a) for spatial reference.

rates promoting low-level instability, and low MLLCL heights meant that the environment was conducive to the formation of tornadoes. While no severe thunderstorm warning was issued for any of these tornadoes, a warning for destructive winds was included in the severe weather statement issued by the BoM, but only after the first few tornadoes were observed on 26 January.

c. East coast low

ECLs commonly affect the NSW and southern QLD coasts each year, particularly during the transition months and winter (Speer et al. 2009). These hybrid systems incorporate both barotropic and baroclinic processes, and are associated with strong low-level shear, appreciable near-surface moisture advection and instability owing to cold upper level support. On 23 February 2013, during the early hours of the morning, an ECL with a low pressure center located over eastern NSW shifted southward (Fig. 5b). For a more detailed case study of this event including radar analysis, readers are directed to Louis (2018). The system produced eight tornadoes as it tracked down the coast (Fig. 5a). This number contrasts the four tornadoes reported by Louis (2018) that focused on

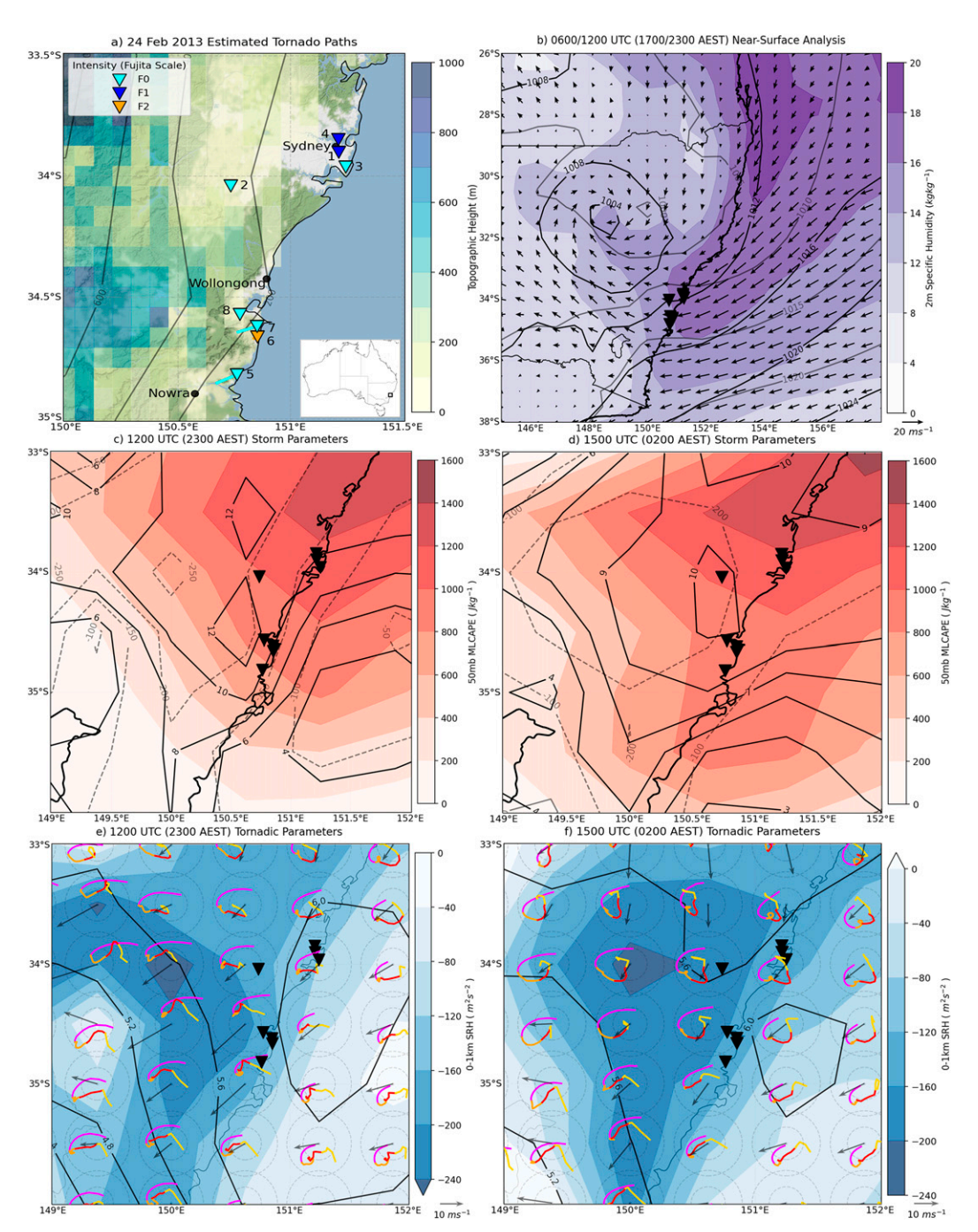


FIG. 5. (a) Distribution of tornado reports by Fujita scale intensity over the south coast of NSW during the landfall of the east coast low for 24 Feb 2013, region relative to Australia inset, and topography as in Fig. 4a. (b) MERRA-2 near-surface analysis of 2 m specific humidity, with 50 m vector winds at 1200 UTC, and sea level pressure at 0600 (gray contours) and 1200 UTC (black contours). (c) MERRA-2 derived storm parameters including 50 hPa mixed-layer CAPE (MLCAPE) at 1200 UTC, with 0–6 km bulk vertical wind shear (S06; black contours), and 0–3 km storm-relative helicity (SRH3; gray dashed). (d) As in (c), but showing storm parameters at 1500 UTC. (e) 1200 UTC tornado parameters SRH1 contours illustrating the strong axis of enhanced near-surface helicity over the region (blue filled contours), with significant tornado parameter for the left mover (STP; dashed contours). Scaled storm-relative hodographs are shown for each grid point as in Fig. 4d. (f) 1500 UTC tornado parameters, displayed as in (e).

TABLE 2. Mean environmental parameters from MERRA-2 proximity soundings for 51 independent cases. Events are classified as F2+ tornado (which may include any class), whether they fit the 850 hPa temperature criteria of warm (WS) or cold season (CS) or alternatively are associated with a tropical cyclone (TC) or east coast low (ECL), and from the pool of events that are WS and CS only, whether they are associated with a discrete supercell. Note that given small sample sizes, mean values should not be considered representative, but rather indicative.

	All	F2+	Supercell	TC	ECL	WS	CS
Sample size	51	6	23	10	6	34	17
850 hPa T (°C)	15.6	15.4	16.7	19.4	14.2	19.3	8.4
SCP (LM)	-2.0	-4.5	-2.1	-3.5	-0.8	-2.5	-1.1
STP (LM)	-0.5	-1.2	-0.4	-1.0	0	-0.6	-0.3
$S01 \text{ (m s}^{-1})$	8.3	14.8	5.9	12.8	10.4	8.6	7.8
$S06 (m s^{-1})$	17.8	22.5	20.0	14.5	9.0	16.3	20.7
$0-1 \text{ km LM SRH } (\text{m}^2 \text{ s}^{-2})$	-86.6	-145	-63.5	-149	-97.8	-100	-59.2
$0-3 \text{ km LM SRH } (\text{m}^2 \text{ s}^{-2})$	-139	-213	-116	-215	-119	-161	-94.5
SBLCL (m)	596	261	1018	123	163	708	371
50 hPa MLLCL (m)	562	269	955	107	150	661	363
100 hPa MLLCL (m)	480	235	832	84	99	588	265
0–3 km lapse rate (°C km ⁻¹)	6.73	6.30	7.59	5.36	6.10	6.73	6.73
2–4 km lapse rate (°C km ⁻¹)	5.96	5.40	6.58	4.77	5.83	5.95	5.97
$700-500 \mathrm{hPa}$ lapse rate (°C km ⁻¹)	5.91	6.06	6.37	4.91	5.73	5.65	6.44
100 hPa MLCAPE (J kg ⁻¹)	769	875	838	969	814	927	454
50 hPa MLCAPE (J kg ⁻¹)	979	1176	984	1385	1064	1193	550
SBCAPE (J kg ⁻¹)	1501	1590	1634	1962	1489	1804	896

formally surveyed high-impact tornadoes; however, each of the eight cases documented in the present study was associated with definable tornadic damage. An onshore moving band of convection associated with a moist plume (most unstable specific humidity of 16–18 g kg⁻¹) from the northeast interacted with the coast, leading to extremely low MLLCLs (less than 300m, not shown), and moderate instability (Figs. 5c,d). At the trailing edge of the band, a southward moving warm front was identifiable from equivalent potential temperature (Louis 2018). This warm front initiated a semidiscrete cluster of cells on its northern edge, producing an environment between 0000 and 0300 AEST characterized by strong S01 (> 15m s^{-1} , not shown), with long cyclonic hodographs increasing the SRH1 to -80 to -160 m² s⁻² (Figs. 5e,f). Combined with steep 0–3 km lapse rates (6 K km⁻¹) and MLCAPE of around 1000 J kg⁻¹, this environment was favorable to tornadoes. However, STP for the region remained zero, primarily due to deep-layer shear (S06) not meeting the 12 m s⁻¹ threshold over the majority of

The tornadoes, located in the coastal region east of the continental divide, ranged from brief F0 events to an F2 tornado between Seven Mile Beach and Nowra (tornado 5; Fig. 5a). Damage paths originating from Seven Mile Beach suggested that at least some of these tornadoes were landfalling tornadic waterspouts that tracked up to 20 km inland. The relative strength of the CAPE environment also likely enhanced the persistence of these cells with the moist onshore flow, though it would appear that many of the low-level characteristics are similar to those found in Oswald (Table 2). This case illustrates a nocturnal tornado risk in Australia and indicates the need for forecasting guidelines and effective warnings (Ashley et al. 2008). It also highlights that the frequently studied ECL systems (Dowdy et al. 2019) that produce both

damaging winds and extreme rainfall hazards may also be associated with a coexistent tornado threat.

d. Supercell tornadoes

On 21 March 2013, a favorable environment for a tornado outbreak (Fig. 6a) developed over northern VIC and southern NSW, driven by cyclogenesis in western Bass Strait (Fig. 6b). The environment was characterized by a narrow moist axis, surface flow from the north backing to northwesterlies at 850 hPa, and a recovering airmass after early day rain.

Seven tornadoes were reported on the day, with the strongest being an F3 observed near Lake Mulwala (tornado 5, Fig. 6a). A cyclic supercell produced this and several other tornadoes near the VIC–NSW border, with extremely long pathlengths (Table A1). This outcome is unsurprising given the environmental conditions favorable for significant tornadoes and relatively fast storm motions (Figs. 6e,f). The parent supercell that produced the F3 tornado was observed in close proximity to the Yarrawonga Doppler radar. Postanalysis of photographic evidence suggests that over the major tornado's path, there were no appropriate damage indicators to substantiate greater than F3 damage. Another track began a small distance to the southeast, traveling toward Rutherglen (tornado 7), suggesting potential for a tornado family; however, without detailed aerial survey, this distinction is not possible.

Analysis of the environmental profiles showed S06 between 25 and 40 m s⁻¹ in the vicinity of the moist axis of the prefrontal trough (Figs. 6b,c), with negative SRH3 increasing with eastward extent favoring left-moving supercells. This favorable shear profile led to appreciable turning from north to northwest, particularly in the 0–1 km layer, resulting in extremely long and looping cyclonic hodographs (Figs. 6d–f). Combined with Bunkers predicted left-moving storm motions to the

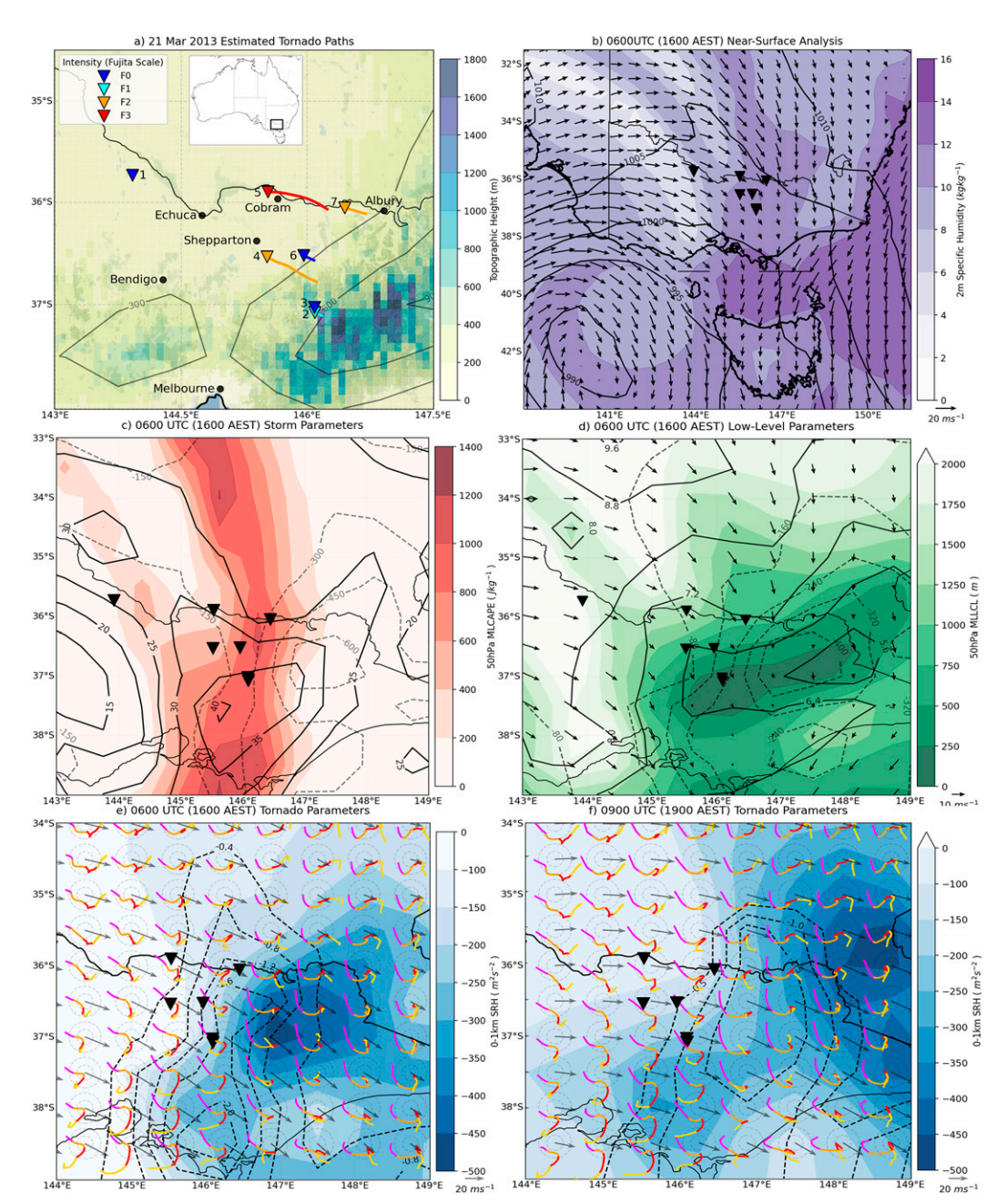


FIG. 6. (a) Distribution of tornado reports by Fujita scale intensity over interior NSW and VIC on the 21 Mar 2013, region relative to Australia inset, and topography as in Fig. 4a. (b) MERRA-2 near-surface analysis of 2 m specific humidity, with 50 m vector winds at 0600 UTC, and sea level pressure at 0600 UTC (black contours). (c) MERRA-2 derived storm parameters including 50 hPa mixed-layer CAPE (MLCAPE) with 0–6 km bulk vertical wind shear (S06; black contours) and 0–3 km storm-relative helicity (SRH3; gray dashed) at 0600 UTC. (d) 50 hPa mixed-layer LCL (MLLCL) with 0–3 km temperature lapse rates (black contours), 0–1 km storm-relative helicity (SRH1; gray dashes), and 50 m wind vectors at 0600 UTC. (e) 0600 UTC tornado parameters SRH1 contours illustrating the strong axis of enhanced near-surface helicity over the region (blue filled contours), with 0–3 km lapse rates (black contours). Scaled storm-relative hodographs are shown for each grid point as in Figs. 4d and 4f, as in (e), but for 0900 UTC.

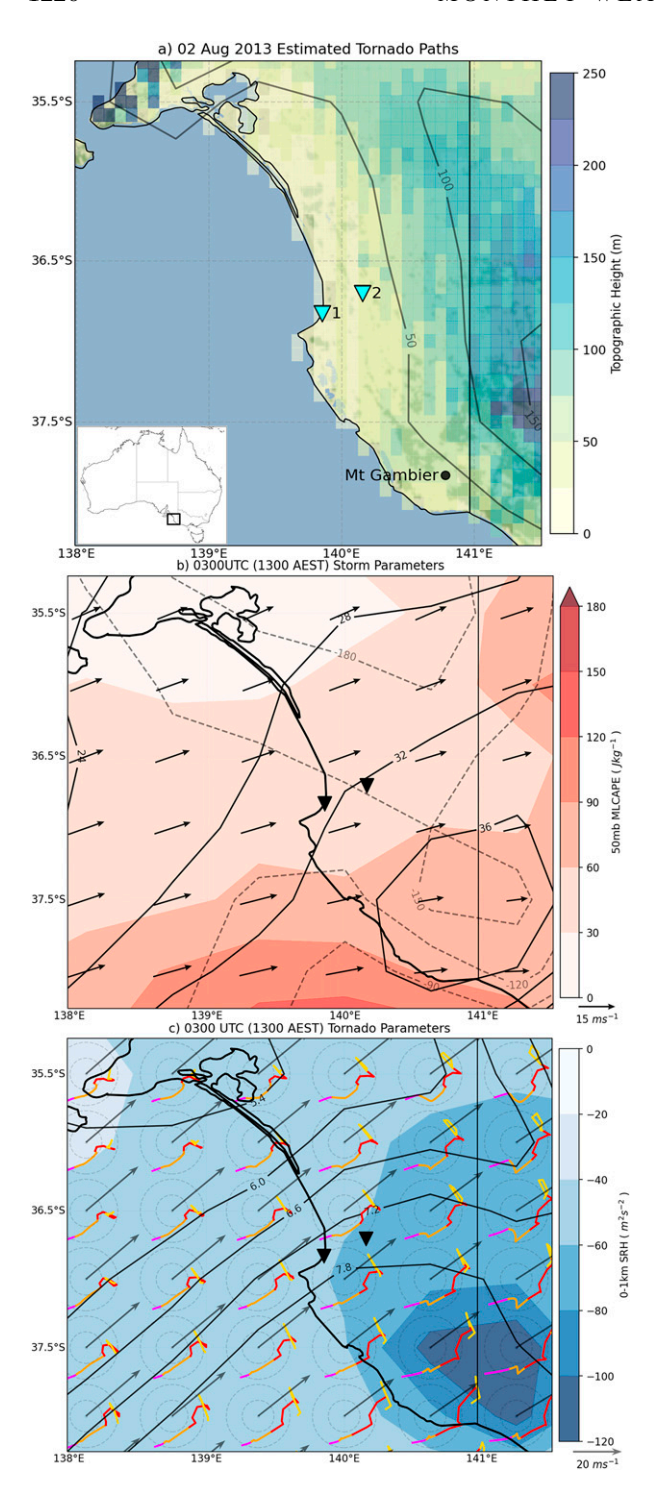


FIG. 7. (a) Distribution of tornado reports by Fujita scale intensity for the cool season event 2 Aug 2013, region relative to Australia inset, and topography as in Fig. 4a, with tornadoes at Kingston (1) and Pealiba (2). (b) MERRA-2 derived storm parameters including 50 hPa mixed-layer CAPE (MLCAPE) with 0–6 km bulk vertical wind shear (S06; black contours) and 0–3 km storm relative helicity (SRH3; gray dashed) at 0300 UTC. (c) 0300 UTC tornado parameters SRH1 contours illustrating the strong axis of enhanced near-surface helicity over the region

southeast, this led to substantive SRH1 between -150 to $-450 \,\mathrm{m}^2 \,\mathrm{s}^{-2}$. However, observed storm motions were slower, and generally east to southeast (with the strongest produced as a storm tracked directly east), which suggests that the helicity realized may have been larger than estimated. Analysis of MLCAPE revealed a very moist near-surface layer, yielding values approaching 1000 J kg⁻¹, perhaps as a result of evaporation from rainfall earlier in the day. The presence of a cloud band for much of the day that cleared to the east prior to storm development assisted in delaying the development of warm sector severe thunderstorms until shear and instability were maximized. Further, this cloud band assisted in moderating the peak surface temperatures, resulting in a higher boundary layer relative humidity, thereby promoting favorable MLLCLs less than 1000 m above ground level, while 0-3 km lapse rates exceeded 7 K km⁻¹ (Fig. 6d). As a result, STP of between -1 and -2 extended through central Victoria from 0600 to 0900 UTC implying favorable conditions for long-track cyclonic F2 + tornadoes and their parent supercells. The narrow moist axis and conditional aspects of this environment made forecasting challenging, as instability dropped off rapidly to the east due to cloud cover, and MLLCLs increased markedly northward with higher surface temperatures. It is also questionable as to whether the profiles determined from MERRA2 are representative, as they exhibit a progressive bias such that the favorable tornado environment had cleared the area when tornadoes were observed at 1900 LT. This bias is evident when comparing the 1600 LT BoM SLP chart to the MERRA2 analysis (Fig. 6b), which suggests the observed prefrontal trough was located farther to the west (not shown).

e. Cool season tornadoes

On 3 August 2013, two cool season tornadoes occurred in SA associated with an extratropical low (Fig. 7a). The cells developed in postfrontal instability resulting from the overlying cold air mass, with MLCAPE of <100 J kg⁻¹, but appreciable 0–3 km lapse rates in excess of 7.2 K km⁻¹ (Figs. 7b,c), a characteristic typical for cool season profiles in the Australian winter (Hanstrum et al. 2002; Mills 2004). Deep layer shear (S06) for the event exceeded 30 m s⁻¹ with a strong mostly unidirectional storm-relative profile (Fig. 7c). S01 and SRH1, however, were not particularly strong, but 0–3 km shear was appreciable, with SRH3 exceeding –120 m² s⁻², suggesting a favorable cool season environment. The conditions led to discrete cell development producing two tornadoes at Kingston (tornado 1) and Keilira (tornado 2).

f. Lower shear and storm mergers

On 23 November 2013, conditions were ripe for supercell formation over northeastern NSW (Fig. 8). Such conditions are

 \leftarrow

(blue filled contours), with 0-3 km lapse rates (black contours). Scaled storm-relative hodographs are shown for each grid point as in Fig. 4d.

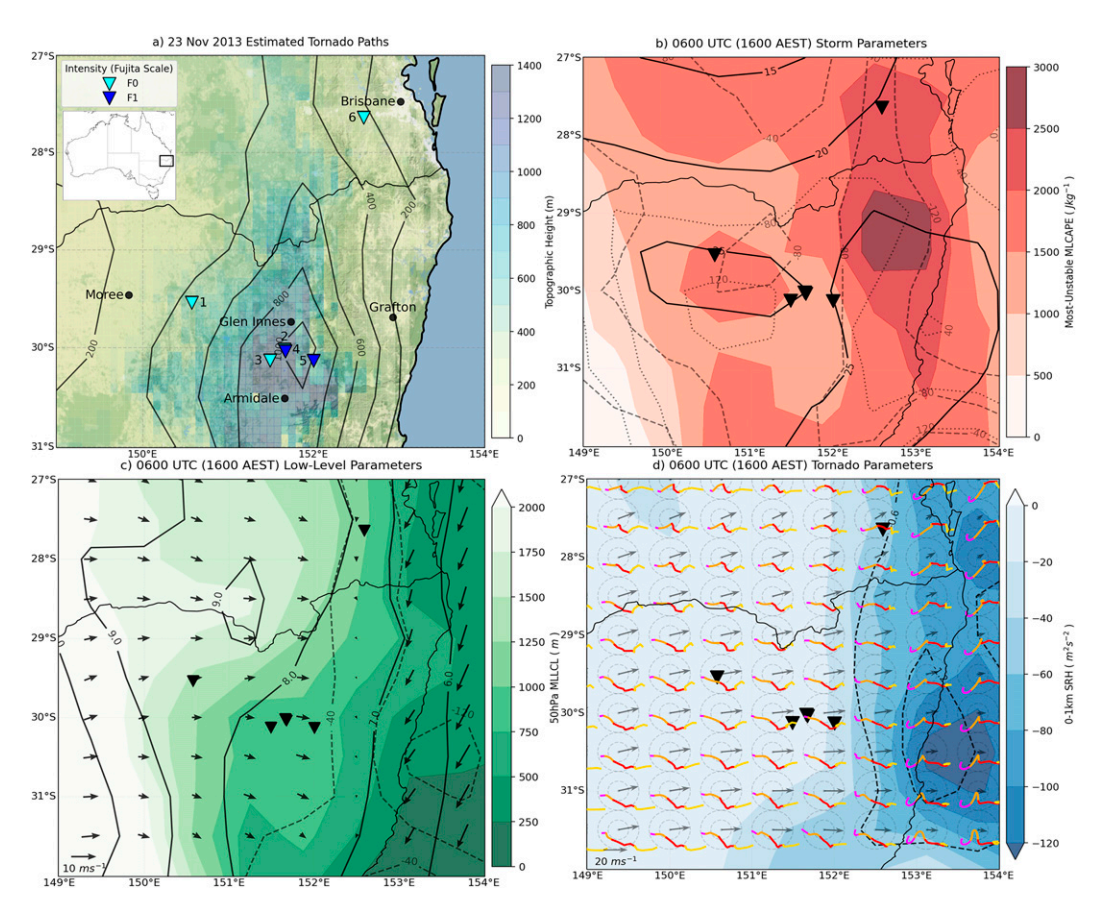


FIG. 8. Distribution of tornado reports by Fujita scale intensity during the northeast NSW tornado outbreak for 23 Nov 2013, with region relative to Australia inset, and topography as in Fig. 4a. (b) MERRA-2 derived storm parameters including most unstable CAPE, with 0–6 km bulk vertical wind shear (S06; black contours), SRH for the left-mover storm motion (gray dashed contours, negative values), and right-moving storm motion (dotted gray contours, positive labels) at 0600 UTC. (c) 50 hPa mixed-layer LCL (MLLCL) with 0–3 km temperature lapse rates (black contours) and 0–1 km storm-relative helicity calculated assuming the left mover as calculated from the internal dynamics method (SRH1; gray dashes) and 50 m wind vectors. (d) 0600 UTC tornado parameters SRH1 contours illustrating the strong axis of enhanced near-surface helicity over the region (blue filled contours), with 0–3 km lapse rates (black contours). Scaled storm-relative hodographs are shown for each grid point as in Fig. 4d.

common during the spring and early summer in this region (Allen and Karoly 2014). The environment was characterized by moderate to strong instability (MUCAPE = $2000-3000 \,\mathrm{J \, kg^{-1}}$), and mostly unidirectional shear producing S06 above 20 m s⁻¹ (Fig. 8b), favoring splitting supercells. Directional shear was limited, evident from the low SRH3 for either storm motion. Numerous cells developed on the edge of the higher terrain in the early afternoon as the cap eroded, and quickly congealed or merged despite several left-moving supercell structures. Morning cloud was likely a key component of the development on the day, restricting daytime heating to a reanalysis maximum of around 20°C; however, in the vicinity of the tornadoes, temperatures observed by a storm chaser were as low as 16°C (M. Bath 2016, personal communication). This, combined with the ample pretrough moisture $(16 \,\mathrm{g \, kg^{-1}})$, contributed to an environment with MLLCLs below 1000 m (Figs. 8c,d). STP was a poor indicator for this event (STP < 0.6), owing to limited SRH. Low-level hodographs for the event were not conducive to tornado development, though farther east toward the coast there was some indication of low-level curvature (magenta, Fig. 8d). Compensating for this limitation, 0–3 km lapse rates were between 7 and 8 K km⁻¹, suggesting that if a supercell storm were to encounter a boundary or other source of low-level helicity, that tornadoes would be possible.

The tornado that affected Warialda (Fig. 8a; tornado 1) was the first reported, associated with a right-moving supercell identified on Namoi radar, in a region of ample bulk shear, modest positive SRH3, and strong instability. The majority of tornadoes in the event were limited to a small geographical area and produced by two storms in the vicinity of the higher terrain between Glen Innes and Armidale (tornadoes 2–5; Fig. 8a). Nearest available radar (Namoi) indicated that storm mergers were occurring at the time that the two strong supercells passed over this vicinity. This suggests that in a favorable supercell environment with low MLLCLs and appreciable

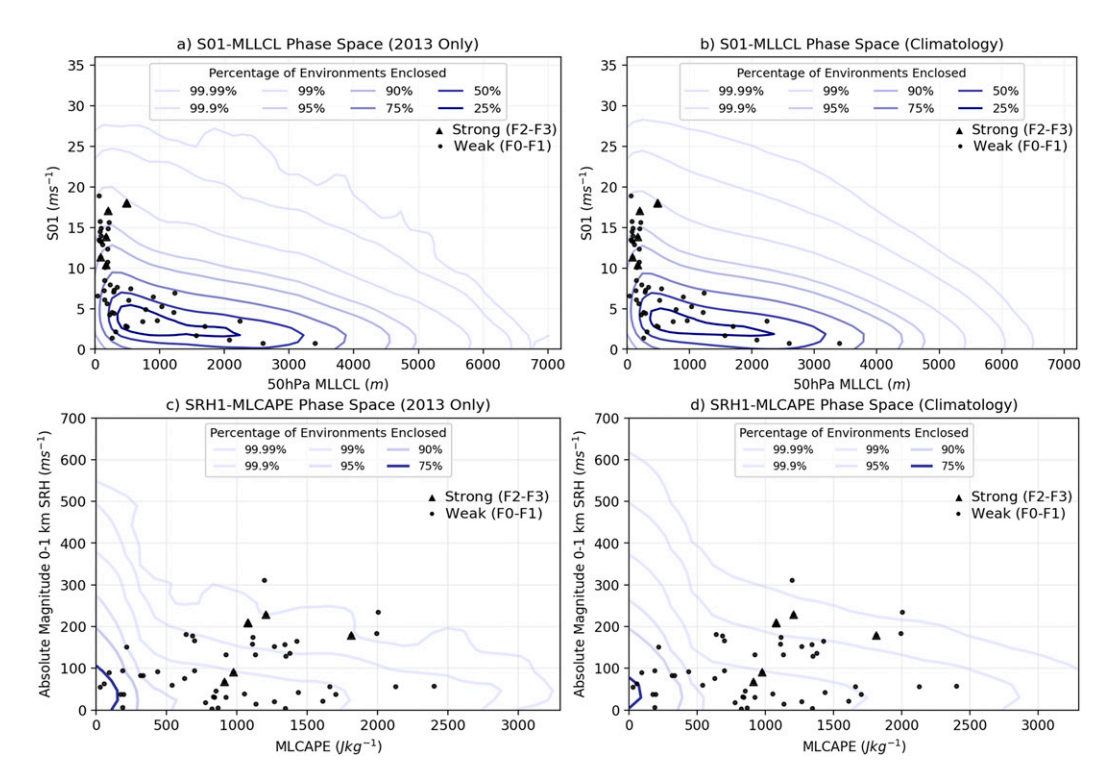


FIG. 9. Kernel-estimated probability density of the respective environmental phase spaces determined based on 2013, and 1980–2019 climatological MERRA-2 environments (contours) as compared to 2013 only observed proximity MERRA-2 environments associated with 2013 observed weak (F0–F1) and strong (F2–F3) tornadoes (symbols) for each plot based on the proximity described in Table 2. (a) 0–1 km shear (S01) and 50 hPa mixed-layer lifting condensation level for environments during 2013 equivalent to Brooks et al. (2003). (b) As in (a), but for phase space for the climatological distribution for 1980–2019. (c) As in (a), but for the absolute magnitude of 0–1 km storm-relative helicity and 50 hPa mixed-layer CAPE equivalent to Brooks et al. (1994). (d) As in (b), but with the same parameters as in (c). Estimates are conditional on nonzero 50 hPa MLCAPE environments and calculated for grid points over land areas exceeding a land–sea mask value of 0.3. Kernel density in terms of log probability density are estimated for a 50 \times 40 x–y bin with a 1.0 Gaussian sigma bandwidth applied. To aid interpretation, these densities are resolved to percentages enclosed by ranking the probabilities at each grid within the phase space, and iteratively finding the normalized probability enclosed at the indicated percentiles of the distribution.

low-level instability, storm mergers, and outflow boundaries likely contributed to a favorable tornado environment at subgrid scale to the analysis. The final tornado of the event (tornado 6) later in the evening was also associated with a cell merging with a squall line, in an environment with appreciable negative SRH1 ($-128\,\mathrm{m^2\,s^{-2}}$) that was likely enhanced by the QLCS. Similar to the Victorian case, it is not clear if the profiles determined from MERRA-2 were representative of the timing of the event.

g. Summary of tornadic environments of 2013

Summarizing these five cases, we explore whether Australia can use U.S. validated composite parameters and thresholds and apply them without adjustment. Three cases were associated with environments were associated with environments that are well known. Tropical cyclone tornadoes (section 3b) are found in many parts of the world (Niino et al. 1997; Onderlinde and Fuelberg 2014; Bai et al. 2020), and the case here follows similar parameters (large 0–3 km lapse rates, strong low-level shear, low MLLCL, STP), with the exception

of the overall 50 hPa MLCAPE being higher. Cool season tornadoes (section 3e) are known to not be well captured by parameters focusing on instability (Hanstrum et al. 2002; Grams et al. 2012; Sherburn et al. 2016), and rather rely on low MLLCL, high low level shear and relative instability, while parameters such as STP are not effective as predictors. It is also clear that supercellular tornado environments are also seen in Australia, with many of the usual U.S. parameters being applicable (section 3d). Characteristics in these cases that appear anomalous are the failure of STP to reveal a meaningful signal in three cases (ECL, cool season tornadoes, low shear, and storm mergers), while other differences include higher 0-3 km lapse rates, and relatively low SRH1. The nocturnal ECL outbreak also highlights the unique nature of these events, with an environment that has lower S06 and substantive 50 hPa MLCAPE as a result of the hybrid structure of these storms.

Extending this analysis to proximity soundings for 2013 tornadoes reveal considerable differences in the distribution of MLLCL-S01 space (Fig. 9a), as compared to the United States and Europe (Brooks et al. 2003; Brooks 2009). A large number

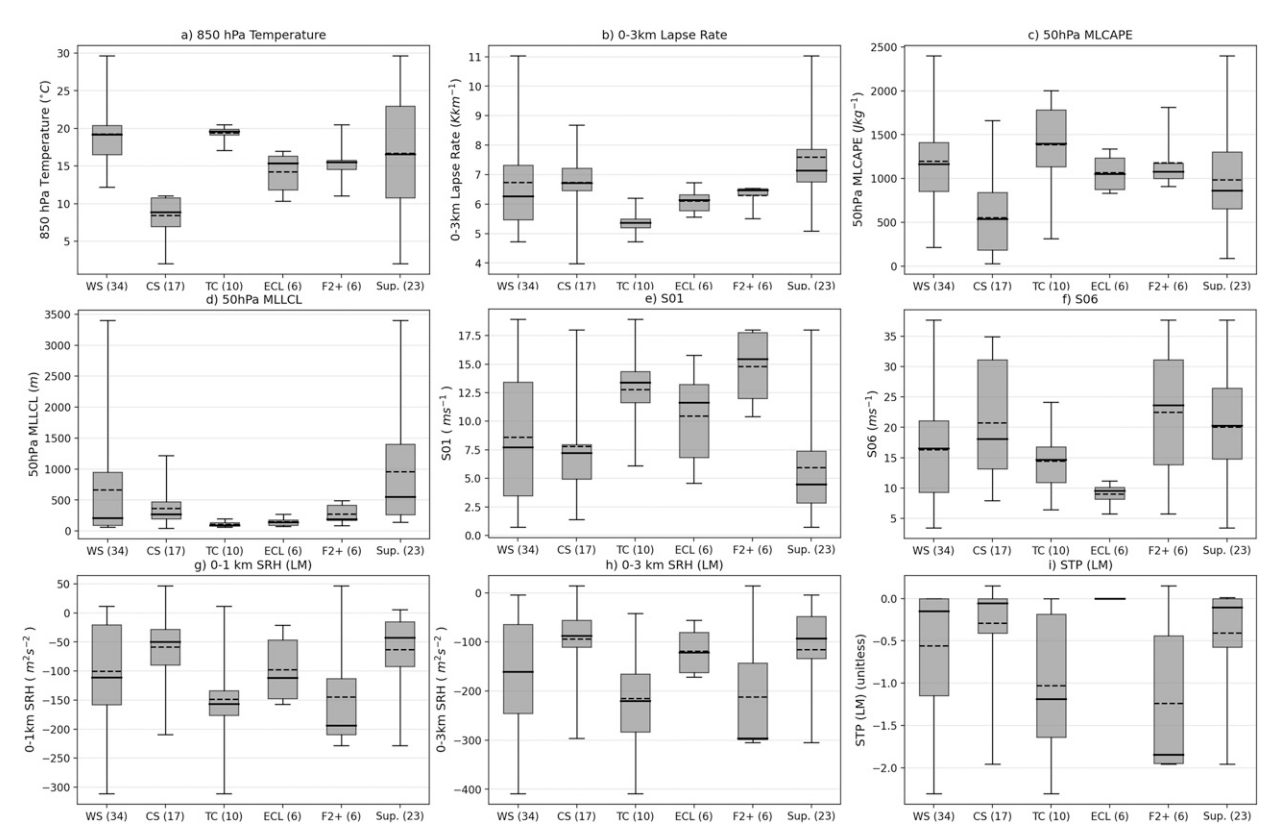


FIG. 10. Distributions of tornado environment parameters from MERRA-2 proximity soundings for 51 independent cases. Events are classified as F2+ tornado (which may include any class), whether they fit the 850 hPa temperature criteria of warm (WS) or cold season (CS) or alternatively are associated with a tropical cyclone (TC) or east coast low (ECL), and from the pool of events that are WS and CS only, whether they are associated with a discrete supercell. The bold line corresponds to median values, while the dashed line reflects the mean, and the box reflects the interquartile range. Whiskers correspond to the absolute range of data. Note that given small sample sizes, values should not be considered representative of all cases, but rather indicative.

of the tornadic cases are associated with MLLCL of less than 500 m, a characteristic rarely seen in the U.S. Great Plains data used by Brooks et al. (2003) (Fig. 10, Table 2). One potential explanation is the considerable difference in environmental parameters between MERRA-2 and the lower-resolution NCEP-NCAR reanalysis used by Brooks et al. (2003). A more likely reasoning, however, is that the environments in Brooks et al. (2003) and Brooks (2009) are biased toward the relatively deep boundary layer mixing environments in the U.S. Great Plains. The 2013 proximity environments have greater similarity to the southeastern United States (Brooks et al. 2003; Grams et al. 2012; Sherburn et al. 2016; King et al. 2017), or perhaps Europe (Taszarek and Kolendowicz 2013; Taszarek et al. 2020). Adding to the complexity is the large number of events (33%) that would be classified as cool season tornadoes (Mills and Colquhoun 1998; Hanstrum et al. 2002), though some of these classifications may be in error over higher terrain. Similarly, TC tornadoes make up a significant fraction (approximately 26%), though with higher instability than found for U.S. cases (McCaul 1991; Edwards 2012). Both of these classes of events are known to be associated with lower MLLCLs (Fig. 10, Table 2). While the sample considered here is comparatively small, Australian tornado events often appear to have S01 above the 7.5 m s⁻¹ threshold (Fig. 10, Table 2) described by Brooks et al. (2003). This is similar to S01 thresholds for tornadoes noted by Taszarek and Kolendowicz (2013), Taszarek et al. (2020), and King et al. (2017). Evaluating the proximity cases relative to the climatological likelihood of nonzero MLCAPE environments in 2013, and relative to longterm climatology (Figs. 9a,b), the proximity profiles do not appear to be outside of the expected frequency. The utility of SRH1 for Australian tornadoes is not as clear cut (Table 2, Fig. 10, Figs. 9c,d), with considerably lower values compared to the right-moving supercell distributions of Coffer et al. (2019). Australian tornadic environments have lower SRH1 for both the strong and weaker tornado cases (Fig. 10), with a significant number of these events occurring in marginal environments $(\leq 100 \,\mathrm{m^2 \, s^{-2}})$. Mean supercell case values are closer to the North American sample, but generally do not see the extreme values. The limited utility of helicity causes issues in applying composite parameters such as supercell composite and STP. In contrast, values for 0-3 km lapse rates are extreme for Australian tornado cases (Table 2, Fig. 10), despite relatively low MLCAPE through the troposphere (Hampshire et al. 2018). Despite the limitations of helicity, the environments that produced known 2013 tornadoes were not exceptional in the

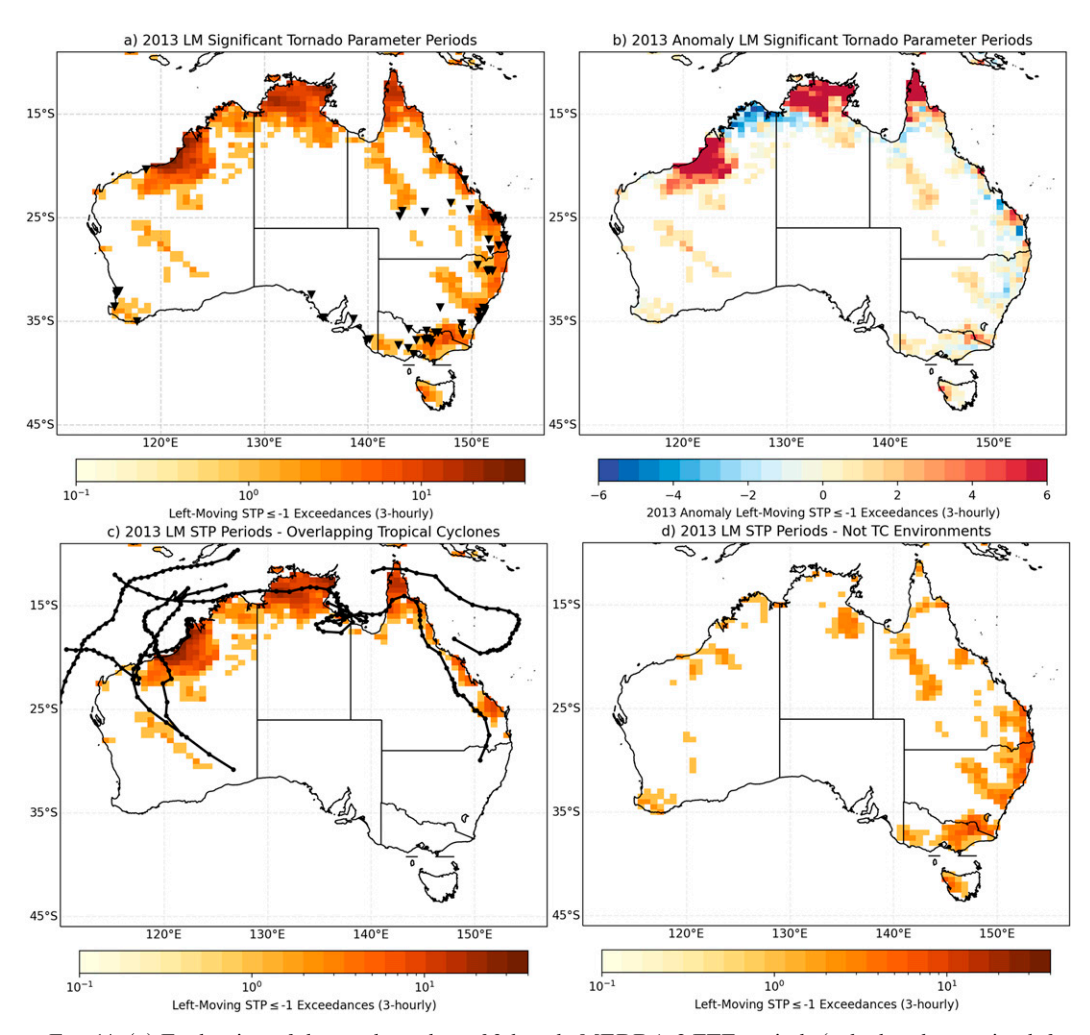


FIG. 11. (a) Evaluation of the total number of 3-hourly MERRA-2 FTE periods (calculated assuming leftmoving storm motions) that occurred during the 2013 calendar year, with observed tornadoes indicated by black triangles. (b) Anomaly of 2013 FTE 3-hourly periods from MERRA2 relative to the 1980–2019 climatology. (c) 3-hourly STP periods on for days coinciding with active tropical cyclones in the Australian basin determined from the IBTrACS dataset (individual storm-track markers show 6-hourly center position, and correspond to the following storms: Christine, Narelle, Oswald, Peta, Rusty, and Tim). Note that not all identified tropical depressions are included within IBTrACS, nor are extratropical transitions, and in light of this, we also include periods with identified depressions (06U and 16U), and tropical lows from the Bureau of Meteorology operational tracks. (d) 3-hourly FTE periods without active tropical cyclones, calculated by subtracting (c) from (a). Note for (a), (c), and(d), a logarithmic scale is used allow for the extreme ranges in frequency.

context of 2013, or as compared to the phase space of the long-term climatology (Figs. 9c,d).

Despite STP having been shown to be imperfect in representing some Australian cases (sections 3c, 3e, and 3f), based on the analysis here it is the only tornadic parameter that appears to capture part of the favorable environmental frequency, and hence we apply it to derive a climatology. Calculating the aggregate 2013 3-hourly periods with STP ≤ -1 for left-moving storms, hereafter, favorable tornado environments (FTEs), yields an estimate of the significant tornado potential over Australia (Fig. 11a). FTEs are spatially collocated with observed tornado cases, despite STP not always being a

reliable indicator. Peak frequency is 5–10 FTEs annually over the east coast, with most locations less than one. The largest differences from 2013 observed tornadoes are over the northern coastline, where FTEs peak. Rich boundary layer moisture and low-level onshore flow is known to inflate convective environment frequency, and this region remains capped most of the year (Allen and Karoly 2014). However, closer examination of these cases reveals that FTEs are generated during periods of landfalling or proximal tropical cyclones (Fig. 11c). High low-level shear and appreciable turning with height in the front-left quadrant of these storms, combined with low lifting condensation levels and at least

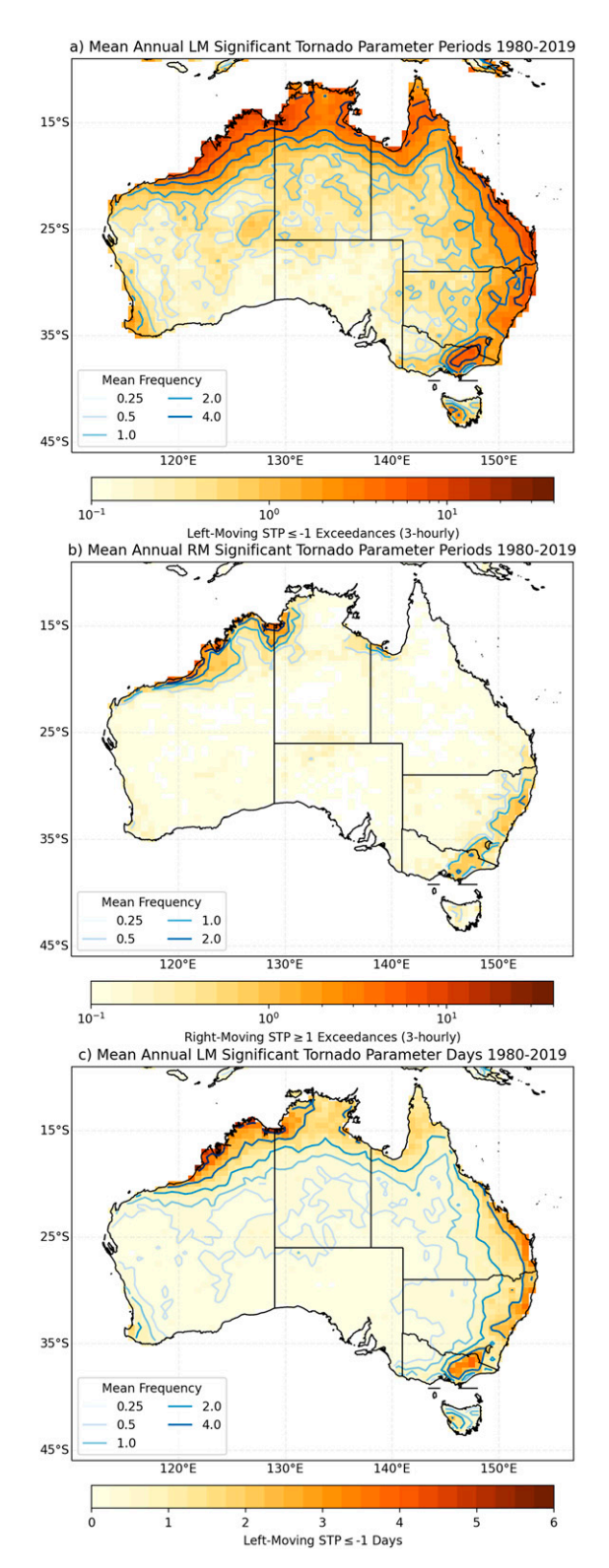


FIG. 12. Mean climatological frequency of FTE periods over Australia from the MERRA-2 climatology 1980–2019. (a) 3-hourly FTE periods estimated using 0–1 km SRH for left-mover storm motions from the internal dynamics method. (b) As in (a), but for right-mover storm motions from the internal dynamics method.

some CAPE results in FTEs (Edwards 2012; Edwards et al. 2012). As ex–Tropical Cyclone Oswald shows, such systems can produce favorable environments for tornadoes both in the outer bands of more intense systems and as remnant systems. This is at least indicative that there is potential for tropical cyclone tornadoes across northern Australia. While the low population density (Fig. 2) means that observations of tornadoes during a tropical cyclone are unlikely, this appears to be an interesting signal for future investigation.

Considered relative to the historical climatology of FTEs (Fig. 12a), 2013 frequencies were not anomalous over most of Australia. These tornadoes fell within regions with at least one FTE every couple of years. The only exception to this are cool season events in SA that are poorly captured by STP (Table 2, Fig. 10). Many events also fall within areas where there are 2–4 FTEs per year. Climatologically, the annual mean frequency of FTEs indicates that the rarest average frequency over the continent is once every 10 years. Areas with at least 1 FTE per year stretch from the coastal fringe northward along the margins of the Great Dividing Range and north to Rockhampton, QLD (Fig. 12a), consistent with the broader distribution of climatological tornado observations (Allen and Allen 2016). Other areas of ≥1 FTE per year are found over the coastal fringe around Perth, WA, and over western TAS. Peak continental values are along the QLD coastal fringe, the coast of northern NSW, and over the highland areas of the Victoria alps. While relatively infrequent compared to the United States (Gensini and Bravo de Guenni 2019), this still constitutes a significant risk. Areas with an FTE every 4 years on average encompass the vast majority of the eastern states, the NT, more than half of WA, and TAS. The tropical cyclone signal is also evident within the full dataset, stretching across the north of the continent. This leads to similar annual averages to the east coast, particularly between Darwin, NT, and the northern parts of WA. Right-moving FTE are also not unprecedented, occurring over similar regions to the left-moving FTE peak with a frequency of at least once every other year. Considering overall frequency as days with one or more FTE reveals that much of the east coast experiences 1-2 days yr⁻¹ with a favorable environment for significant tornadoes.

While these climatological distributions are revealing, we emphasize the sample cannot be considered representative. Nevertheless, our results suggest the need to consult a wider dataset of observed tornado to environment relationships for the evaluation of forecast parameters for Australia (Doswell 2007) and to enhance our understanding of tornado climatology. The favorable environment maps for 2013 suggest it is likely that a greater number of tornadoes may have occurred than are reported here.

 \leftarrow

(c) As in (a), but instead using the number of FTE days. Blue contours are used to emphasize delineations in frequency and gradient over the background logarithmic scale.

4. Discussion

a. Observations

Observation of tornadoes in Australia is challenging given the large area of the continent with low population density and uneven distribution (e.g., Geerts and Noke-Raico 1995; Allen and Allen 2016). Despite this, the number of tornadoes being reported in the BoM STA database for 2013 [37; 9 of the 46 original reports were not independent tornadoes; BOM (2020)] is still significantly less than the number of crossvalidated observations (69) available from nontraditional sources, such as social media, news reports, and weather discussion boards. This suggests the potential to retrospectively expand the climatology of Australian tornadoes in the historical record (e.g., Allen and Allen 2016), or at least begin inclusion of these alternate sources moving forward in order to have a more accurate understanding of Australian tornado occurrence.

Few of the 2013 tornadoes were surveyed by the BoM (southeast NSW coast (Louis 2018); northeast VIC; northeast NSW, Ipswich, Warwick, QLD), while a large number of events do not appear in the BoM STA tornado database (Table A1). This is often despite being confirmed as tornadoes in statements to the press. Metadata for all tornadoes was extremely limited, even in cases where surveys were conducted not all metadata were entered in the STA. Limited resources and service prioritization toward general operations, and perceptually greater hazards such as flooding, bushfires and tropical cyclones (Munro 2011) mean that finding staff trained to conduct surveys is challenging. To address this challenge, the authors recommend prioritizing surveying significant events, and encouraging local observers and/or using online resources to substantiate a tornado observation. Actively collating this data would then provide the necessary visual evidence and site survey details that would otherwise be unobtainable, and could include drone flyovers of paths similar to Soderholm et al. (2020a). This approach would be sufficient to retrieve damage path width and length, and to determine the tornado's strength in lieu of survey resources. Guidance for the damage ratings of tornadoes is also necessary to minimize subjectivity of individual surveyors. The lack of transferable structural damage indicators between U.S. and Australian building codes and vegetation types mean that the EF-scale is not trivial to apply. Similar problems have arisen in rating tree damage in the United States from region to region, and these limitations also warrant careful consideration (Peterson 2007; Edwards et al. 2013). While global efforts are underway to rectify the cross-applicability of the EF-scale (J. LaDue 2019, personal communication), a formal policy is needed. We stress that while there will always be limits to resources, it is imperative to ensure the quality of the tornado database is maintained by surveying reported tornadoes to allow development of forecasting guidelines, as has been seen in the United States (Edwards et al. 2013).

b. Forecasting guidelines

Synoptic environments favorable to tornado development can be similar across many parts of the globe, however, frequency of these environments can vary (Brooks 2009, 2013; Taszarek et al. 2020). For example, when comparing the United States and Europe, for the same environment the likelihood of a significant tornado increases in Europe owing to enhanced forcing. This also highlights an important consideration; it is plausible that tornadic environments exist in Australia that may rarely occur elsewhere (Brooks 2013; Allen and Allen 2016).

As has been illustrated by the selected cases (section 3), tornadoes in Australia are found in a range of regimes, some of which overlap with known conditions in the United States, suggesting that existing forecast parameters may be useful. The tornadic environments present across the 69 Australian tornado cases in 2013 also occur in the United States, but the total of 1392 U.S. tornadoes per annum (annual average 2005-19) suggests that these tornadic environments are more frequent there. Nonetheless, these occurrences are frequent enough to justify developing specific forecasting guidelines for Australia. While utilizing guidelines for other countries may be a starting point, more observations are needed to develop thresholds for Australian conditions, or verify that those used overseas are applicable to local climatic conditions. Australia's most intense tornadoes (mostly F2) are not frequently studied in the United States, given the focus on case studies that produce even stronger tornadoes. This presents an opportunity to expand our understanding of these more marginal environments and construct climatologies to better understand their occurrence.

c. The warning process

The occasional frequency of tornadoes in Australia as revealed through studying 2013 raises the question as to whether there is any value in warning for tornadoes for the continent. Currently, negative lead times are generally associated with the few tornado warnings issued in Australia. This does not reflect the evolution of the technology, such as the growing Doppler radar coverage, with 24 C- or S-Band units (SREP 2015; BOM 2017), especially given more are to be deployed in the near future. Such a challenge is not unique to Australia, as tornadoes go unwarned over much of Europe and elsewhere (Rauhala and Schultz 2009).

Warning systems in Australia are similarly not designed for warning specifically for tornadoes, and can encompass a variety of hazards (damaging winds, large hail, heavy rainfall, and tornadoes). Using the same warning for all of these hazards can lead to public consternation upon experiencing a tornado when the storm was under a general or lifted severe thunderstorm warning (The New Daily 2015). However, while rare, tornado warnings for Australia are not unprecedented, with several recent cases referring to more specific tornado risk in a broader severe thunderstorm warning. In most of these cases, these warnings stemmed from observed ongoing tornadoes, or where a storm had a history of producing tornadoes and had a strong mesocyclone on Doppler radar. Tornadoes are also not a BoM priority as compared to bushfires, flooding and tropical cyclones. For example, in the Munro (2011) review of the bureau's capacity to respond to future extreme weather and natural disasters, tornadoes were not mentioned anywhere in the 122-page document. Other challenges are posed by how

warnings for tornadoes can be incorporated within broader messaging for larger-scale damaging wind storms when appropriate (e.g., ECLs, tropical cyclones), or when waterspouts move onshore. Finally, despite the evident hazard from climatology, we note that tornado warnings may also not resonate with the Australian public, similar to the challenges noted in Europe (Rauhala and Schultz 2009). Based on limited sampling, the population is not fully aware that tornadoes occur in Australia (Keul et al. 2018). Of those that are aware of these events, common perception is that tornadoes are weaker in Australia than those occurring in the United States, and thus do not pose a significant threat. Thus, even assuming an appropriate warning issuance, there remains a public credibility issue, and it is unclear whether they would be prepared to deal with advice given; e.g., finding appropriate shelter. Despite this, examples of the infiltration of North American advice for sheltering for a tornado via mainstream media (i.e., sheltering in a windowless central room) have been identified in cases where the public observed a tornado prior to its impact on their home or building.

5. Conclusions

Tornadoes in 2013 have been used to present a case for threat posed by these events in Australia. The 69 tornadoes that occurred were interrogated in the context of the existing historical climatology, and explored using proxy environments to estimate the underlying hazard. This illustrated that 2013 was observationally anomalous, and environmentally less than remarkable outside of the tropical cyclone region. Compared to the incomplete observed record, frequency appears anomalously high, but is spatially consistent with known historical locations of tornado occurrence. Applying the significant tornado parameter as a proxy, climatology shows that favorable tornado environments regularly occur along the east and north coast of the continent at least a few days a year on average. Farther inland, the frequency drops to once every 2–4 years, and 2013 environments here are more of an anomaly from the long-term average. Hence, 2013 was likely not anomalous outside of northern Australia where a significant number of tropical cyclones made landfall. Five short case studies were explored to illustrate the diversity of formative environments found in Australia and highlight the need for forecast guidelines encompassing a range of conditions. These included tornado outbreaks associated with an east coast low, in the cool season, in a low-helicity storm merger environment and with the passage of an ex-tropical cyclone. Finally, the issues associated with observations, forecasting and warnings for tornado events were discussed in relation to the identified climatological risk.

Australian tornadoes offer unique opportunities for study. For example, half of the Australian continent is closer to the equator than any part of the United States or Europe, and includes tropical regimes, which suggests that known tornado environments may not capture the conditions favorable to storms in these areas. This is not to say that all environments are unique, for example cool season tornadoes, which are similar between California and southern

Australia, and arguably also the southeastern United States (26%, Table 1; Hanstrum et al. 2002; Mills 2004; Richter 2007; Kounkou et al. 2009; Sherburn and Parker 2014; Sherburn et al. 2016). The evidence presented here suggests that tornadoes occur with Australian tropical cyclones similar to other basins worldwide and should be investigated further (Niino et al. 1997; Onderlinde and Fuelberg 2014; Jones et al. 2019; Bai et al. 2020). Tornadoes are also found to occur in the subtropical region, and are associated with the hybrid ECL systems, regimes that are not commonly found in other locations where climatologies of tornadoes have been assessed.

The authors reiterate that increasing knowledge of tornadoes in Australia is far from simple. Addressing the limitations of the current warning system, enhancing observational records and updating forecast guidelines will assist in providing an effective warning system, but will not change public perception of tornado risk in Australia. What is clear from the results here is that these perceptions are misplaced. A true climatology of events and risk is the first step needed to summarize the threat, and the presence of a threat communicated effectively to the general public. As exposure to the hazard will only increase with time in response to increasing population and urban sprawl, it is highly plausible a predictable tornado event will impact a heavily populated area in Australia without warning.

Acknowledgments. This material is based upon work supported by the National Science Foundation under Grant AGS-1945286. C. Lepore's contribution is based upon work support by the National Science Foundation under Grant OCE-1740648. The authors are grateful for comments by Robert Warren and Dean Sgarbossa during internal review and Cameron Nixon for his contribution of the hodograph mapping approach. The views expressed within this article are solely those of the authors and not the Australian Bureau of Meteorology. The authors appreciate the insightful suggestions provided by the reviewers that improved the clarity and content of the manuscript.

Data availability statement. Historical tornado data are sourced from the Bureau of Meteorology Severe Thunderstorm Archive (STA) (BOM 2020). Identified tornado cases and metadata in this study are provided in Table A1, with further metadata and copies of source information available from the authors by request. Radar data used were accessed via The Weather Chaser (2017). MERRA-2 data used produce convective output are publicly available from the Global Modeling and Assimilation Office (GMAO) at the NASA Goddard Space Flight Center (Gelaro et al. 2017). Owing to the size of the postprocessed reanalysis dataset, these data are available by email request to the authors.

APPENDIX

2013 Tornado Records

As a larger number of events were identified that did not appear within the BoM STA (BOM 2020), records were

season (CS). This classification was only applied in cases where a tornado was not associated with a tropical cyclone (TC) or east coast low (ECL). Storm mode was broken down for WS indicates that the time is unknown. Radar verifications and classification correspond to reflectivity (R), velocity (V), both (R/V), and outside of coverage (OC). Path width and length are in meters based on survey or thorough analysis of documentary evidence. Season is determined based on the 850 hPa temperatures exceeding or below 12°C as warm season (WS) or cool and CS cases into either tornadoes associated with a radar-determined supercell (Supercell) as left-moving supercell (LM Sup.), supercell but motion not clear (Sup.), right-moving TABLE A1. List of all observed tornadoes occurring in Australia during 2013, and whether they were included in the BoM STA. Time is given in HHMM format using AEST, and UNK supercell (RM Sup.), or disorganized (Disorg.) including quasi-linear convective systems and nonsupercellular cases. Tropical cyclone supercell (TC Sup.) and ECL mesocyclonic (ECL Meso) are kept as a separate category. Tornado likelihood is determined as described in the appendix section as unconfirmed (U), likely (L), or definite (D).

145.47 Weak (F0) — — — WS 143.06 Weak (F0) — — — WS 143.29 Weak (F1) — — — WS 115.56 Weak (F1) — — — WS 146.97 Weak (F1) — — — WS 146.97 Weak (F1) — — — WS 149.29 Weak (F1) — — — — TC 149.29 Weak (F1) — — — TC 152.44 Weak (F1) — — — TC 152.48 Weak (F1) — — — TC 152.49 Weak (F1) — — — TC 152.41 Weak (F0) — — — TC 152.42 Weak (F0) — — — TC 152.43 Weak (F0) — — — TC 152.54 Weak (F0) — — — TC 152.54 Weak (F0) — — — TC 152.55 Weak (F0) — — — TC 152.57 Weak (F1) — — — TC 152.61 Weak (F1) — — — TC 152.62 Weak (F1) — — — — TC 152.63 Weak (F1) — — — — TC 152.64 Weak (F1) — — — — — CC 152.76 Weak (F1) — — — — — CC 152.76 Weak (F1) — — — — — CC 152.76 Weak (F1) — — — — — CC 152.76 Weak (F1) — — — — — CC 153.13 Weak (F1) — — — — — CC 153.13 Weak (F1) — — — — — — ECL 150.74 Weak (F1) — — — — — — ECL 150.75 Weak (F1) — — — — — — ECL 150.76 Weak (F1) — — — — — — — ECL 150.77 Weak (F1) — — — — — — ECL 150.78 Weak (F1) — — — — — — — — — — ECL 150.78 Weak (F1) — — — — — — — — — — — — — — — — — — —	Radar STA	STA		State	Nearest location	Lat	Lon	Rating	Length	Width	Injuries	Season	Mode	Likelihood
143.06 Weak (F0) — WS 143.29 Weak (F0) — — WS 115.56 Weak (F1) — — WS 118.61 Weak (F1) — — WS 146.97 Weak (F0) — — WS 146.97 Weak (F0) — — WS 149.29 Weak (F0) — — WS 152.44 Weak (F1) — — — TC 152.48 Weak (F1) — — — WS 152.49 Weak (F1) — — — WS 152.49 Weak (F1) — — — TC 152.40 Weak (F1) — — — TC 152.44 Weak (F1) — — — TC 152.49 Weak (F1) — — — TC 152.41 Weak (F1) — — — TC 152.52 Weak (F1) — — — TC	2050 R No QLD Blackall	No QLD	QTD	Blackall		-24.42	145.47	Weak (F0)	I		Ι	WS	LM Sup.	Γ
143.29 Weak (F0) — WS 115.56 Weak (F1) — WS 118.61 Weak (F1) — WS 146.97 Weak (F1) — WS 147.47 Weak (F0) — — WS 149.29 Weak (F1) — — TC 152.44 Weak (F1) — — TC 152.48 Weak (F1) — — TC 152.49 Weak (F1) — — — TC 152.49 Weak (F1) — — — TC 152.40 Weak (F1) — — — TC 152.44 Weak (F1) — — — TC 152.49 Weak (F1) — — — TC 152.41 Weak (F0) — — — TC 152.52 Weak (F1) — — — TC 152.54 Weak (F1) — — — TC 150.74 Weak (F1) —	R Yes QLD	Yes QLD	QLD	Jundah		-24.83	143.06	Weak (F0)	I	I	l	MS	LM Sup.	О
115.56 Weak (F1) — — — WS 118.61 Weak (F1) — — — WS 118.61 Weak (F1) — — — WS 146.97 Weak (F0) — — — WS 149.29 Weak (F1) — — — — WS 152.44 Weak (F1) — — — — TC 152.48 Weak (F1) — — — TC 152.49 Weak (F1) — — — TC 152.41 Weak (F1) — — — TC 152.41 Weak (F0) — — — TC 152.53 Weak (F0) — — — TC 152.53 Weak (F0) — — — TC 152.57 Weak (F0) — — — TC 152.58 Weak (F1) — — — TC 152.59 Weak (F1) — — — TC 152.50 Weak (F1) — — — TC 152.61 Weak (F1) — — — TC 152.75 Weak (F1) — — — TC 152.76 Weak (F1) — — — — TC 152.76 Weak (F1) — — — — TC 152.76 Weak (F1) — — — — CS 152.76 Weak (F1) — — — — WS 151.21 Weak (F1) — — — — ECL 151.22 Weak (F1) 1000 — — ECL 151.24 Weak (F1) 1600 — ECL 151.25 Weak (F1) 1600 — ECL 151.26 Weak (F1) 1600 — ECL 152.27 Weak (F1) 1600 — ECL 152.38 Weak (F1) 1600 — ECL 153.38 Weak (F1) 1600 — FCL 153.78 Weak (F1) — — — — HCL 153.78 Weak (F1) — — — — — HCL 153.78 Weak (F1) — — — — — HCL 153.78 Weak (F1) — — — — — HCL 153.78 Weak (F1) — — — — — HCL 153.78 Weak (F1) — — — — — — — HCL 153.78 Weak (F1) — — — — — — — — HCL 153.78 Weak (F1) — — — — — — — — HCL 153.78 Weak (F1) — — — — — — — — — — — HCL 153.78 Weak (F1) — — — — — — — — — — — — — — — — — — —	R No QLD Sto	No OLD	QLD	Stonehenge		-24.35	143.29	Weak (F0)				WS	LM Sup.	Ω
118.61 Weak (F1) — — WS 146.97 Weak (F0) — — WS 146.97 Weak (F0) — — — WS 147.47 Weak (F0) — — — WS 149.29 Weak (F1) — — — TC 152.46 Strong (F2) 1500 400 17 TC 152.41 Weak (F1) — — — TC 152.48 Weak (F1) — — — TC 152.49 Weak (F1) — — — TC 152.40 Weak (F1) — — — WS 152.41 Weak (F1) — — — WS 152.53 Weak (F1) — — — — TC 152.54 Weak (F1) — — — TC 152.55 Weak (F1) — — — TC 152.76 Weak (F1) — — — TC <td< td=""><td>R/V Yes WA</td><td>Yes WA</td><td>WA</td><td>Capel</td><td></td><td>-33.55</td><td>115.56</td><td>Weak (F1)</td><td> </td><td> </td><td> </td><td>MS</td><td>LM Sup.</td><td>О</td></td<>	R/V Yes WA	Yes WA	WA	Capel		-33.55	115.56	Weak (F1)				MS	LM Sup.	О
146.97 Weak (F0) — — WS 147.47 Weak (F0) — — — WS 147.47 Weak (F1) — — — WS 149.29 Weak (F1) — — — TC 152.46 Strong (F2) 1500 400 17 TC 152.41 Weak (F1) — — — TC 152.48 Weak (F1) — — — TC 152.49 Weak (F1) — — — TC 152.40 Weak (F1) — — — WS 152.41 Weak (F1) — — — WS 152.53 Weak (F0) — — — TC 152.54 Weak (F1) — — — TC 152.55 Weak (F1) — — — TC 153.75 Weak (F1) — — — TC 152.76 Weak (F1) — — — TC <td< td=""><td>R No WA F</td><td>No WA</td><td>WA</td><td>Karlgarin</td><td></td><td>-33.55</td><td>118.61</td><td>Weak (F1)</td><td>I</td><td>l</td><td>l</td><td>MS</td><td>LM Sup.</td><td>О</td></td<>	R No WA F	No WA	WA	Karlgarin		-33.55	118.61	Weak (F1)	I	l	l	MS	LM Sup.	О
147.47 Weak (F0) — 200 — TC 149.29 Weak (F1) — — — TC 149.31 Weak (F1) — — — TC 152.46 Strong (F2) 1500 400 17 TC 152.41 Weak (F1) — — — TC 152.48 Weak (F1) — — — TC 152.48 Weak (F1) — — — TC 152.48 Weak (F1) — — — TC 149.01 Weak (F0) — — — TC 152.48 Weak (F0) — — — WS 153.12 Weak (F0) — — — — TC 152.59 Weak (F1) — — — — TC 153.13 Weak (F1) — — — — TC 153.24 Weak (F1) — — — — — TC 150.24 Weak (F1	R Yes	Yes NSW	NSM	Ungarie		-33.64	146.97	Weak (F0)		I		MS	Sup.	Ω
149.29 Weak (F1) — — — TC 149.31 Weak (F0) — — — TC 152.46 Strong (F2) 1500 400 17 TC 152.41 Weak (F1) — — — TC 152.48 Weak (F1) — — — TC 152.48 Weak (F0) — — — TC 152.49 Weak (F0) — — — TC 152.41 Weak (F0) — — — Wo 153.12 Weak (F0) — — — TC 152.59 Weak (F1) 10000 200 4 TC 152.61 Weak (F1) — — — CS 153.13 Weak (F1) — — — TC 153.24 Weak (F1) — — — — CS 150.74 Weak (F1) 1000 — — Wo 150.54 Weak (F1) 1600 10 ECL <td>R Yes</td> <td>Yes QLD</td> <td>OLD</td> <td>Inkerman</td> <td></td> <td>-19.69</td> <td>147.47</td> <td>Weak (F0)</td> <td>I</td> <td>200</td> <td>I</td> <td>1C</td> <td>TC Sup.</td> <td>О</td>	R Yes	Yes QLD	OLD	Inkerman		-19.69	147.47	Weak (F0)	I	200	I	1 C	TC Sup.	О
149.31 Weak (F0) — — — TC 152.46 Strong (F2) 1500 400 17 TC 152.41 Weak (F1) — — — TC 152.48 Weak (F1) — — — TC 152.07 Weak (F0) — — — TC 149.01 Weak (F0) — — — TC 152.41 Weak (F0) — — — TC 153.12 Weak (F0) — — — TC 152.59 Weak (F1) 10000 200 4 TC 152.50 Weak (F1) — — — CS 153.13 Weak (F1) — — — TC 152.59 Weak (F1) — — — TC 153.13 Weak (F1) — — — TC 153.24 Weak (F1) — — — — Was 150.24 Weak (F1) 1600 100 —	R No	No QLD	QLD	Hay Point		-21.31	149.29	Weak (F1)	I	I	I	1 C	TC Sup.	Ω
152.46 Strong (F2) 1500 400 17 TC 152.48 Weak (F1) — — — — TC 152.48 Weak (F1) — — — — TC 152.07 Weak (F0) — — — — TC 149.01 Weak (F0) — — — — WS 152.41 Weak (F0) — — — — WS 152.42 Weak (F0) — — — — TC 153.12 Weak (F0) — — — — TC 153.13 Weak (F1) 10000 200 4 TC 153.14 Weak (F1) — — — TC 153.15 Weak (F1) — — — TC 153.16 Weak (F1) — — — ECL 153.17 Weak (F1) — — — ECL 153.18 Weak (F1) — — — — WS 153.19 Weak (F1) — — — WS 154.24 Weak (F1) — — — ECL 150.24 Weak (F1) — — — ECL 150.24 Weak (F1) — — — ECL 150.25 Weak (F1) — — — ECL 150.26 Weak (F1) — — — ECL 150.27 Weak (F1) — — — ECL 150.28 Weak (F1) = — — — ECL 150.28 Weak (F1) = — — — ECL 150.29 Weak (F1) = — — — ECL 150.29 Weak (F1) = — — — ECL 150.27 Weak (F1) = — — — ECL 150.28 Weak (F1) = — — — ECL 150.28 Weak (F1) = — — — ECL 150.38 Weak (F1) = — — — ECL 150.38 Weak (F1) = — — — ECL 150.38 Weak (F1) = — — — ECL	R No	No QLD	QLD	Grasstree Beach		-21.36	149.31	Weak (F0)	I		I	1 C	TC Sup.	О
152.41 Weak (F1) — — — — TC 152.48 Weak (F1) — — — — TC 152.07 Weak (F0) — — — — TC 149.01 Weak (F0) — — — — TC 153.12 Weak (F1) — — — — TC 153.13 Weak (F0) — — — — TC 153.13 Weak (F1) — — — — TC 153.14 Weak (F1) — — — — TC 153.15 Weak (F1) — — — TC 153.17 Weak (F1) — — — TC 153.18 Weak (F1) — — — TC 153.19 Weak (F1) — — — TC 153.10 Weak (F1) — — — TC 153.11 Weak (F1) — — — TC 153.12 Weak (F1) — — — CS 154.13 Weak (F1) — — — WS 154.14 Weak (F1) — — — ECL 156.15 Weak (F1) — — — ECL 156.15 Weak (F1) — — — ECL 156.15 Weak (F1) — — — ECL 157.24 Weak (F1) — — — ECL 157.25 Weak (F1) — — — ECL 157.26 Weak (F1) — — — ECL 157.27 Weak (F1) — — — ECL 157.28 Weak (F1) — — — ECL 157.39 Weak (F1) — — — — ECL 157.30 Weak (F1) — — — — ECL 157.31 Weak (F1) — — — ECL 157.32 Weak (F1) — — — — ECL 157.33 Weak (F1) — — — — ECL 157.34 Weak (F1) — — — — ECL 157.35 Weak (F1) — — — — ECL	R Yes	Yes QLD	QLD	Bargara		-24.82	152.46	Strong (F2)	1500	400	17	$^{\mathrm{LC}}$	TC Sup.	О
152.48 Weak (F1) — — — TC 152.07 Weak (F0) — — — — TC 149.01 Weak (F0) — — — — TC 152.41 Weak (F1) — — — — — WS 152.42 Weak (F1) — — — — TC 153.12 Weak (F0) — — — — TC 153.13 Weak (F1) — — — — TC 153.14 Weak (F1) — — — TC 152.15 Weak (F1) — — — TC 152.16 Weak (F1) — — — TC 152.17 Weak (F1) — — — TC 153.18 Weak (F1) — — — TC 153.19 Weak (F1) — — — ECL 151.21 Weak (F1) — — — ECL 150.24 Weak (F1) — — — ECL 150.24 Weak (F1) — — — ECL 150.25 Weak (F1) — — ECL 150.26 Weak (F1) — — ECL 150.27 Weak (F1) 1600 100 — ECL 150.28 Weak (F1) 1600 100 — ECL 150.28 Weak (F1) 1600 75 — ECL 150.78 Weak (F1) 8000 75 — ECL 150.78 Weak (F1) 8000 75 — ECL 150.78 Weak (F1) — — — ECL	R Yes	Yes QLD	QLD	Burnett Heads		-24.77	152.41	Weak (F1)				TC	TC Sup.	Ω
152.07 Weak (F0) — — — TC 149.01 Weak (F0) — — — — TC 152.41 Weak (F1) 14400 — 2 TC 153.12 Weak (F0) — — — TC 153.13 Weak (F0) — — — TC 153.13 Weak (F1) — — — TC 152.14 Weak (F1) — — — TC 152.15 Weak (F1) — — — TC 152.16 Weak (F1) — — — TC 152.17 Weak (F1) — — — TC 153.18 Weak (F1) — — — TC 153.19 Weak (F1) — — — TC 153.19 Weak (F1) — — — TC 153.10 Weak (F1) — — — TC 153.11 Weak (F1) — — — CS 153.12 Weak (F1) — — — WS 153.13 Weak (F1) — — — WS 153.14 Weak (F1) — — — ECL 153.15 Weak (F1) — — — ECL 153.16 Weak (F1) — — — ECL 153.17 Weak (F1) — — — ECL 153.18 Weak (F1) — — — ECL 153.19 Weak (F1) — — — — ECL	R Yes	Yes QLD	QLD	Coonarr		-24.96	152.48	Weak (F1)		I		$^{\mathrm{LC}}$	TC Sup.	О
149.01 Weak (F0) — — WS 152.41 Weak (F1) 14400 — — WS 153.12 Weak (F0) — — — TC 152.59 Weak (F0) — — — TC 153.13 Weak (F0) — — — TC 152.61 Weak (F1) — — — TC 152.76 Weak (F1) — — — TC 143.87 Weak (F1) — — — CS 134.53 Weak (F1) — — — WS 151.21 Weak (F1) — — — WS 150.74 Weak (F1) 1000 — — WS 150.74 Weak (F1) — — WS 150.85 Weak (F1) 1600 100 — WS 150.66 Strong (F2) 15700 250 — ECL 1 150.78 Weak (F1) — — — WS ECL </td <td>R Yes</td> <td>Yes QLD</td> <td>QLD</td> <td>Bungadoo</td> <td></td> <td>-24.98</td> <td>152.07</td> <td>Weak (F0)</td> <td>I</td> <td>I</td> <td>I</td> <td>1C</td> <td>TC Sup.</td> <td>О</td>	R Yes	Yes QLD	QLD	Bungadoo		-24.98	152.07	Weak (F0)	I	I	I	1 C	TC Sup.	О
152.41 Weak (F1) 14400 — 2 TC 153.12 Weak (F0) — — — — TC 153.13 Weak (F0) — — — — TC 153.13 Weak (F0) — — — — TC 152.61 Weak (F1) — — — — TC 152.61 Weak (F1) — — — — TC 152.76 Weak (F1) — — — — TC 143.87 Weak (F1) — — — — CS 134.53 Weak (F1) — — — — WS 151.21 Weak (F1) — — — — WS 151.22 Weak (F1) — — — ECL 150.74 Weak (F1) 3410 — ECL 150.75 Weak (F1) 1600 — ECL 150.76 Weak (F1) 1600 — ECL 150.77 Weak (F1) 1600 — ECL 150.78 Weak (F1) — — — ECL	R No	No ACT	ACT	West Macgregor		-35.21	149.01	Weak (F0)	I	I	I	WS	Sup.	Д
153.12 Weak (F0) — — — TC 152.59 Weak (F0) 1500 160 — TC 153.13 Weak (F0) — — — TC 152.61 Weak (F1) — — — TC 152.61 Weak (F1) — — — TC 152.76 Weak (F1) — — — TC 143.87 Weak (F1) — — — CS 134.53 Weak (F1) — — — CS 151.21 Weak (F1) — — — ECL 151.22 Weak (F1) 1000 — 1 ECL 150.74 Weak (F1) 3410 — ECL 150.74 Weak (F1) 1600 — ECL 150.75 Weak (F1) 1600 — ECL 150.76 Weak (F1) 1600 — ECL 150.77 Weak (F1) 1600 — ECL 150.78 Weak (F1) — — — ECL	R Yes	Yes QLD	QLD	Burnett Heads		-24.77	152.41	Weak (F1)	14400	I	7	1 C	TC Sup.	Ω
152.59 Weak (F0) 1500 160 — TC 153.13 Weak (F0) — — — — TC 152.61 Weak (F1) 10000 200 4 TC 152.76 Weak (F1) — — — — TC 143.87 Weak (F1) — — — — CS 134.53 Weak (F1) — — — — WS 151.21 Weak (F1) — — — — WS 151.22 Weak (F1) 1000 — 1 ECL 150.74 Weak (F1) 3410 — ECL 150.74 Weak (F1) 3410 — ECL 150.75 Weak (F1) 1600 — ECL 150.76 Weak (F1) 1600 — ECL 150.77 Weak (F1) 1600 100 — ECL 150.78 Weak (F1) 1500 75 — ECL 150.78 Weak (F1) 1500 75 — ECL 150.78 Weak (F1) — — — ECL	V No QLD Mooloolabah	No QLD Mooloolabah	QLD Mooloolabah			-26.68	153.12	Weak (F0)	I	I	I	1 C	TC Sup.	О
153.13 Weak (F0) — — — TC 152.76 Weak (F1) 10000 200 4 TC 152.76 Weak (F1) — — — TC 143.87 Weak (F1) — — — CS 134.53 Weak (F1) — — — CS 151.21 Weak (F0) — — — WS 151.22 Weak (F1) 1000 — 1 ECL 151.23 Weak (F1) 3410 — ECL 151.24 Weak (F0) — ECL 152.46 Weak (F0) — ECL 153.26 Weak (F1) 3410 — ECL 153.27 Weak (F1) 3410 — ECL 153.28 Weak (F1) 3410 — ECL 153.29 Weak (F1) 3410 — ECL 153.246 Weak (F1) — ECL 150.28 Weak (F1) 1600 100 — ECL 150.28 Weak (F1) 1600 75 — ECL 150.78 Weak (F1) 1600 75 — ECL 150.78 Weak (F1) — — ECL	R/V Yes QLD Burrum Heads	Yes QLD Burrum Heads	QLD Burrum Heads			-25.23	152.59	Weak (F0)	1500	160	I	1 C	TC Sup.	Ω
3 152.61 Weak (F1) 10000 200 4 TC 1 152.76 Weak (F1) — — TC 1 143.87 Weak (F0) — — CS 134.53 Weak (F0) — — CS 151.21 Weak (F0) — — WS 151.22 Weak (F1) 1000 — ECL 1 151.22 Weak (F1) 3410 — — ECL 1 151.22 Weak (F0) — — — ECL 1 151.22 Weak (F0) — — WS 152.46 Weak (F0) — — WS 150.85 Weak (F1) 1600 100 — ECL 1 150.78 Weak (F1) 15700 250 — ECL 1 150.78 Weak (F1) — — — HCI 1 150.78 Weak (F1) — — — HCI 1 150.78 Weak (F1) <	V No	No QLD	QLD	Bribie Island		-26.99	153.13	Weak (F0)	I	I	l	1 C	TC Sup.	D
152.76 Weak (F1) — — — TC 143.87 Weak (F0) — — — CS 134.53 Weak (F0) — — — CS 151.21 Weak (F0) — — — WS 151.22 Weak (F1) 1000 — 1 ECL 151.22 Weak (F1) 3410 — ECL 151.22 Weak (F0) — — ECL 152.46 Weak (F0) — — ECL 150.85 Weak (F1) 1600 100 — ECL 150.85 Weak (F1) 1600 100 — ECL 150.86 Strong (F2) 15700 250 — ECL 150.78 Weak (F1) — — — WS 150.78 Weak (F1) 1600 100 — ECL 150.79 FCL	R Yes	Yes QLD	QLD	Burrum Heads		-25.18	152.61	Weak (F1)	10000	200	4	1 C	TC Sup.	О
143.87 Weak (F0) — — — CS 134.53 Weak (F1) — — — WS 151.21 Weak (F0) — 100 — ECL 151.25 Weak (F1) 1000 — 1 ECL 150.74 Weak (F1) 3410 — ECL 151.22 Weak (F0) — — ECL 151.24 Weak (F0) — — ECL 150.85 Weak (F1) 1600 100 — ECL 150.85 Weak (F1) 15700 250 — ECL 150.78 Weak (F1) — — — WS	R/V Yes	Yes QLD D	QLD D	Dundowran Beach		-25.27	152.76	Weak (F1)	I		I	1 C	TC Sup.	О
134.53 Weak (F1) — — WS 151.21 Weak (F0) — 100 — ECL 151.25 Weak (F1) 1000 — 1 ECL 150.74 Weak (F1) 3410 — — ECL 151.22 Weak (F0) — — ECL 151.24 Weak (F0) — — ECL 150.85 Weak (F1) 1600 100 — ECL 150.85 Weak (F1) 1600 100 — ECL 150.87 Weak (F1) 15700 250 — ECL 150.78 Weak (F1) — — ECL 150.78 Weak (F1) 15700 100 — ECL 150.78 Weak (F1) — — ECL	R/V No VIC	No VIC	VIC	Ballarat		-37.56	143.87		I	I	I	CS	Disorg.	О
5 151.21 Weak (F0) — 100 — ECL 151.25 Weak (F1) 1000 — 1 ECL 151.22 Weak (F1) 3410 — ECL 151.22 Weak (F0) — — ECL 151.22 Weak (F0) — — — ECL 151.246 Weak (F0) — — — WS 150.85 Weak (F1) 1600 100 — ECL 150.85 Weak (F1) 1600 100 — ECL 150.85 Weak (F1) 1500 250 — ECL 150.78 Weak (F1) — — — — ECL 150.78 Weak (F1) — — — ECL 150.78 Weak (F1) — — — — — ECL 150.78 Weak (F1) — — — — — ECL 150.78 Weak (F1) — — — — — — ECL 150.78 Weak (F1) — — — — — — ECL 150.78 Weak (F1) — — — — — — — ECL 150.78 Weak (F1) — — — — — — ECL 150.78 Weak (F1) — — — — — — — — ECL 150.78 Weak (F1) — — — — — — — — — — — ECL 150.78 Weak (F1) — — — — — — — — — — — — — — — — — — —	R Yes	Yes SA	SA	Wirrulla		-32.4	134.53	Weak (F1)				WS	LM Sup.	О
5 151.25 Weak (F1) 1000 — 1 ECL 1 150.74 Weak (F1) 3410 — ECL 1 151.22 Weak (F0) — — ECL 1 2 152.46 Weak (F0) — — WS 1 150.85 Weak (F1) 1600 100 — ECL 1 150.6 Strong (F2) 15700 250 — ECL 1 5 150.78 Weak (F1) — — ECL 1 5 150.78 Weak (F1) — — ECL 1	V No	No NSW	NSW	Kirrabilli		-33.85	151.21	Weak (F0)	I	100	I	ECL	ECL Meso	О
150.74 Weak (F1) 3410 — — ECL 151.22 Weak (F0) — — — ECL 151.24 Weak (F0) — — — — WS 152.46 Weak (F1) 1600 100 — ECL 150.85 Weak (F1) 1600 100 — ECL 150.6 Strong (F2) 15700 250 — ECL 150.78 Weak (F1) — — — — — — ECL 150.78 Weak (F1) — — — — — ECL 150.78 Weak (F1) — — — — — — ECL 150.78 Weak (F1) — — — — — — ECL 150.78 Weak (F1) — — — — — — ECL 150.78 Weak (F1) — — — — — — ECL 150.78 Weak (F1) — — — — — — — ECL 150.78 Weak (F1) — — — — — — — — ECL 150.78 Weak (F1) — — — — — — — — — — — ECL 150.78 Weak (F1) — — — — — — — — — — — — — — — — — ECL 150.78 Weak (F1) — — — — — — — — — — — — — — — — — — —	V No NSW	No NSW	NSW	Malabar		-33.96	151.25	Weak (F1)	1000	I	1	ECL	ECL Meso	О
151.22 Weak (F0) — — — — ECL 15.246 Weak (F0) — — — — — WS 152.46 Weak (F1) 1600 100 — — — WS 150.78 Weak (F1) 15700 250 — ECL 150.78 Weak (F1) 8000 75 — ECL 150.78 Weak (F1) — — — — ECL 150.78 Weak (F1) — — — — ECL 150.78 Weak (F1) — — — ECL 150.78 Weak (F1) — — — — — ECL 150.78 Weak (F1) — — — — — ECL 150.78 Weak (F1) — — — — — — ECL 150.78 Weak (F1) — — — — — — ECL 150.78 Weak (F1) — — — — — — ECL 150.78 Weak (F1) — — — — — — ECL 150.78 Weak (F1) — — — — — — — ECL 150.78 Weak (F1) — — — — — — — ECL 150.78 Weak (F1) — — — — — — — — ECL 150.78 Weak (F1) — — — — — — — — ECL 150.78 Weak (F1) — — — — — — — — ECL 150.78 Weak (F1) — — — — — — — — — — — — — — — — — — —	NSN ON 1	No NSW	NSW	Narellan		-34.04	150.74	Weak (F1)	3410		I	ECL	ECL Meso	О
152.46 Weak (F0) — — WS 150.85 Weak (F1) 1600 100 — ECL 1 150.6 Strong (F2) 15700 250 — ECL 1 150.78 Weak (F1) 8000 75 — ECL 1 150.78 Weak (F1) — — ECL 1	V No	No NSW	NSW	Moore Park		-33.9	151.22	Weak (F0)	I	I	I	ECL	ECL Meso	Д
150.85 Weak (F1) 1600 100 — ECL 1 150.6 Strong (F2) 15700 250 — ECL 1 150.78 Weak (F1) 8000 75 — ECL 1 150.78 Weak (F1) — — ECL 1	R No QLD	No QLD	QLD	Bargara		-24.82	152.46	Weak (F0)	I	I	I	MS	Disorg.	О
150.6 Strong (F2) 15700 250 — ECL 1 150.78 Weak (F1) 8000 75 — ECL 1 150.78 Weak (F1) — — ECL 1	V Yes NSW	Yes NSW	NSW	Kiama		-34.67	150.85	Weak (F1)	1600	100	I	ECL	ECL Meso	Д
150.78 Weak (F1) 8000 75 — ECL 1 150.78 Weak (F1) — — ECT 1	V Yes NSW Nowra/S	Yes NSW Nowr	NSW Nowr			-34.87	150.6	Strong (F2)	15700	250	I	ECL	ECL Meso	О
150 78 Weak (F1) — — FCI	V Yes	Yes NSW	NSM	Jamberoo		-34.65	150.78	Weak (F1)	8000	75	I	ECL	ECL Meso	О
130:10 Mcda (11)	No No	No NSW	MSM	Albion Park		-34.57	150.78	Weak (F1)	I		I	ECL	ECL Meso	Q

TABLE A1. (Continued)

						IABLE	ABLE AI. (Commueu)	inuea)						
Date	Time	Radar	STA	State	Nearest location	Lat	Lon	Rating	Length	Width	Injuries	Season	Mode	Likelihood
21 Mar	1530	R	Yes	VIC	Kerang	-35.73	143.92	Weak (F0)	I		I	WS	LM Sup.	D
	1810	R/V	Yes	VIC	Mansfield	-37.05	146.09	Weak (F1)	I	I	I	CS	LM Sup.	D
	1830	R/V	Yes	VIC	Mansfield	-37.05	146.09	Weak (F0)			I	S	LM Sup.	D
	1830	R/V	Yes	VIC	Violettown	-36.64	145.72	Strong (F2)	I	100	1	WS	LM Sup.	О
	1850	R/V	Yes	VIC	Cobram/Mulwala	-35.92	145.65	Strong (F3)	00009	250	100	WS	LM Sup.	О
	1930	R/V	Yes	VIC	Euroa	-36.75	145.48	Weak (F0)	I	100	0	WS	LM Sup.	О
	2010	R/V	Yes	VIC	Rutherglen	-36.06	146.46	Strong (F2)	I	I	I	WS	LM Sup.	D
23 Apr	1535	R/V	Yes	QLD	Emerald/Anakie	-23.54	147.99	Weak (F0)	I	I	I	MS	LM Sup.	D
	1700	R	Yes	OLD	Baralaba	-24.19	149.83	Weak (F1)	I	100	I	MS	LM Sup.	D
o Jun	0090	R	No	WA	Elleker	-35.01	117.73	Weak (F0)	I	I	I	CS	Sup.	L
12 Jun	2100	R	Yes	OLD	Pratten/Warwick	-28.09	151.78	Weak (F1)	30000	100	1	WS	Sup.	D
25 Jun	0530	R	No	WA	Port Hedland	-20.31	118.58	Weak (F1)			I	WS	LM Sup.	D
4 Jul	0090	0C	Yes	SA	Big Swamp	-34.64	135.7	Weak (F0)	I	I	I	S	Sup.	О
7 Jul	2000	R/V	Yes	VIC	Knowsley	-36.81	144.66	Weak (F0)	400	I	I	CS	LM Sup.	L
15 Jul	1120	R	Š	VIC	Swan Pool	-36.74	146	Weak (F1)	I	100	I	CS	Disorg.	J
21 Jul	UNK	0C	No	VIC	Mansfield	-37.05	146.09	Weak (F0)	I	I	I	CS	Disorg.	D
	UNK	0C	No	VIC	Mansfield	-37.05	146.09	Weak (F0)	I	I		CS	Disorg.	D
3 Aug	1240	R	Yes	SA	Kingston	-36.83	139.85	Weak (F1)	1500	20	I	CS	Sup.	D
	1300	R	No	SA	Keilira	-36.7	140.16	Weak (F1)	I	I	I	CS	Sup.	О
6 Aug	1414	R	No	WA	North Coogee	-32.09	115.76	Weak (F1)	I	I	9	CS	Sup.	D
21 Aug	1730	R/V	Yes	SA	Waterloo Corner	-34.73	138.58	Weak (F1)	200	20	I	CS	Sup.	О
11 Sep	0200	R	No	WA	Secret Harbour	-32.41	115.75	Weak (F1)	I	I		CS	Sup.	О
$16 \operatorname{Sep}$	1945	R	No	OLD	Maclagan	-27.08	151.63	Weak (F1)	I	150		WS	Disorg.	О
22 Sep	0300	×	No	WA	Ellamere Retreat	-32.05	116.01	Weak (F1)		75	I	S	Sup.	D
22 Oct	1900	R/V	No	VIC	Barnawartha North	-36.07	146.74	Weak (F1)	I	I	I	WS	LM Sup.	J
	1930	R	No	VIC	Ararat	-37.28	142.93	Strong (F2)	200	40		CS	LM Sup.	О
16 Nov	0630	R/V	No	OLD	Moreton Island	-27.09	153.42	Weak (F0)	I	I	I	WS	LM Sup.	О
$18 \mathrm{Nov}$	1415	R/V	No	NSM	Fairlight	-33.8	151.28	Weak (F0)	1750			ECL	ECL Meso	О
	1445	R/V	Yes	NSW	Hornsby	-33.7	151.1	Weak (F1)	2500	20	15	ECL	ECL Meso	О
$19 \mathrm{Nov}$	0300	R	Yes	OLD	Urangan	-25.28	152.9	Weak (F1)	I	30		WS	LM Sup.	О
23 Nov	1520	R	No	NSW	Warialda	-29.54	150.57				I	WS	RM Sup.	D
	1600	R	Yes	NSW	Ben Lomond/Maybole	-30.02	151.66		I	200	I	S	LM Sup.	О
	1630	R	Yes	NSW	Tenterden Rd	-30.13	151.49	Weak (F1)	4000	175		MS	LM Sup.	О
	1630	R	Yes	NSW	Tingha	-30.04	151.67	Weak (F0)	1000	100		CS	LM Sup.	Д
	1700	R	Yes	NSW	Bald Blair	-30.13	152.01	Weak (F0)	2400	09	I	S	LM Sup.	О
	2000	R/V	N _o	OLD	Rosewood	-27.64	152.59	Weak (F1)	2000	I	I	MS	LM Sup.	О
	1230	R/V	No	VIC	Batesford	-38.15	144.35		I	I	I	S	Disorg.	О
26 Dec	1550	R/V	Yes	NSM	Cooma	-36.24	149.13	Weak (F0)			1	CS	LM Sup.	D

supplemented using an adaptive keyword search process. Initial reference terms included: "thunderstorm," "storm," "damage," "tornado," "mini-tornado," "cyclone," "hail," and "wind," which were applied independently and in combination for the search, along with restricting the search to the calendar year 2013. Once locations experiencing candidate storms were identified, these location names and dates were comprehensively scrutinized for all digital media forms, and where available, eyewitness accounts. A similar approach was applied to all listed 2013 STA tornado and wind cases to cross-validate their occurrence and add metadata. These two approaches revealed a substantive number of media articles for storm cases though not limited to tornadoes. The criteria sought for each tornado case built off the approach of Evesson (1970) and Allen (1980), namely: observation or visual evidence of a funnel cloud co-occurring with damage, structural damage resulting in the substantive transport of debris outside of the structure, treefall that was not in unidirectional alignment, tops of trees snapped off, carrying of debris for long distances or observed in the air by those present, narrow paths of damage, unusually severe structural damage, isolated damage along storm path and the description of a roar or jet engine consistent with one or more of the above. Each case that met one or more of these criteria were then assessed using radar data, where available, to identify whether a mesocyclone or organized storm was present. Observations that included direct observation of the tornado, or evidence was emphatic such that a tornado was the most likely cause were classified as definite. Likely cases met one or more of the criteria listed above, but either lacked firsthand observations or visual evidence of the tornado. Four cases were uncertain due to lack of evidence of a defined ground damage path despite evidence otherwise indicating a tornado. The resulting tornado dataset used within this study is detailed in Table A1.

REFERENCES

- Allen, J. T., and D. J. Karoly, 2014: A climatology of Australian severe thunderstorm environments 1979–2011: Inter-annual variability and ENSO influence. *Int. J. Climatol.*, 34, 81–97, https://doi.org/10.1002/joc.3667.
- —, and E. R. Allen, 2016: A review of severe thunderstorms in Australia. *Atmos. Res.*, **178–179**, 347–366, https://doi.org/ 10.1016/j.atmosres.2016.03.011.
- —, D. J. Karoly, and G. A. Mills, 2011: A severe thunderstorm climatology for Australia and associated thunderstorm environments. *Aust. Meteor. Oceanogr. J.*, 61, 143–158, https:// doi.org/10.22499/2.6103.001.
- Allen, S., 1980: A Preliminary Australian Tornado Climatology. Bureau of Meteorology, 15 pp.
- Ashley, W. S., A. J. Krmenec, and R. Schwantes, 2008: Vulnerability due to nocturnal tornadoes. *Wea. Forecasting*, **23**, 795–807, https://doi.org/10.1175/2008WAF2222132.1.
- Bai, L., Z. Meng, K. Sueki, G. Chen, and R. Zhou, 2020: Climatology of tropical cyclone tornadoes in China from 2006 to 2018. Sci. China Earth Sci., 63, 37–51, https://doi.org/ 10.1007/s11430-019-9391-1.
- BOM, 2017: Bureau of Meteorology radar network. Australian Bureau of Meteorology, accessed 2 August 2017, http://www.bom.gov.au/australia/radar/.

- —, 2020: Bureau of Meteorology severe thunderstorm archive. Australian Bureau of Meteorology, accessed 10 July 2020, http://www.bom.gov.au/australia/stormarchive/.
- Boustead, J. M., B. E. Mayes, W. Gargan, J. L. Leighton, G. Phillips, and P. N. Schumacher, 2013: Discriminating environmental conditions for significant warm sector and boundary tornadoes in parts of the Great Plains. Wea. Forecasting, 28, 1498–1523, https://doi.org/10.1175/WAF-D-12-00102.1.
- Brooks, H. E., 2009: Proximity soundings for severe convection for Europe and the United States from reanalysis data. *Atmos. Res.*, **93**, 546–553, https://doi.org/10.1016/j.atmosres.2008.10.005.
- —, 2013: Severe thunderstorms and climate change. Atmos. Res., 123, 129–138, https://doi.org/10.1016/j.atmosres.2012.04.002.
- —, C. A. Doswell III, and J. Cooper, 1994: On the environments of tornadic and nontornadic mesocyclones. *Wea. Forecasting*, 9, 606–618, https://doi.org/10.1175/1520-0434(1994)009<0606: OTEOTA>2.0.CO:2.
- —, J. W. Lee, and J. P. Craven, 2003: The spatial distribution of severe thunderstorm and tornado environments from global reanalysis data. *Atmos. Res.*, 67–68, 73–94, https://doi.org/ 10.1016/S0169-8095(03)00045-0.
- Bunkers, M. J., B. A. Klimowski, J. W. Zeitler, R. L. Thompson, and M. L. Weisman, 2000: Predicting supercell motion using a new hodograph technique. *Wea. Forecasting*, **15**, 61–79, https://doi.org/10.1175/1520-0434(2000)015<0061:PSMUAN> 2.0.CO;2.
- Clarke, R. H., 1962: Severe local wind storms in Australia. Rep. 13, Commonwealth Scientific and Industrial Research Organization, Australia, 56 pp.
- Coffer, B. E., M. D. Parker, R. L. Thompson, B. T. Smith, and R. E. Jewell, 2019: Using near-ground storm relative helicity in supercell tornado forecasting. *Wea. Forecasting*, 34, 1417–1435, https://doi.org/10.1175/WAF-D-19-0115.1.
- Deslandes, R., H. Richter, and T. Bannister, 2008: The end-to-end severe thunderstorm forecasting system in Australia: Overview and training issues. *Aust. Meteor. Mag.*, **57**, 329–343.
- Doswell, C. A., 2007: Small sample size and data quality issues illustrated using tornado occurrence data. *Electron. J. Severe Storms Meteor.*, **2** (5), https://ejssm.org/ojs/index.php/ejssm/article/viewArticle/26/27.
- ——, H. E. Brooks, and N. Dotzek, 2009: On the implementation of the enhanced Fujita scale in the USA. *Atmos. Res.*, 93, 554– 563, https://doi.org/10.1016/j.atmosres.2008.11.003.
- Dowdy, A. J., and Coauthors, 2019: Review of Australian East Coast low pressure systems and associated extremes. *Climate Dyn.*, **53**, 4887–4910, https://doi.org/10.1007/s00382-019-04836-8.
- Edwards, R., 2012: Tropical cyclone tornadoes: A review of knowledge in research and prediction. *Electron. J. Severe Storms Meteor.*, **7** (6), https://ejssm.org/ojs/index.php/ejssm/article/viewArticle/97.
- —, A. R. Dean, R. L. Thompson, and B. T. Smith, 2012: Convective modes for significant severe thunderstorms in the contiguous United States. Part III: Tropical cyclone tornadoes. Wea. Forecasting, 27, 1507–1519, https://doi.org/10.1175/ WAF-D-11-00117.1.
- —, J. G. LaDue, J. T. Ferree, K. Scharfenberg, C. Maier, and W. L. Coulbourne, 2013: Tornado intensity estimation: Past, present, and future. *Bull. Amer. Meteor. Soc.*, 94, 641–653, https://doi.org/10.1175/BAMS-D-11-00006.1.
- Evesson, D., 1970: Tornado occurrences in New South Wales. *Aust. Meteor. Mag.*, **17**, 143–165.
- Fox-Hughes, P., I. Barnes-Keoghan, and A. Porter, 2018: Observations of a tornado at an Automatic Weather Station in northern

- Tasmania. J. Southern Hemisphere Earth Syst. Sci., 68, 215–230, https://doi.org/10.1071/ES18012.
- Fujita, T. T., 1971: Proposed characterization of tornadoes and hurricanes by area and intensity. Satellite and Mesometeorology Research Project, Department of the Geophysical Sciences, University of Chicago, 48 pp.
- ——, 1973: Tornadoes around the world. Weatherwise, 26, 56–83, https://doi.org/10.1080/00431672.1973.9931633.
- Garner, J., 2013: A study of synoptic-scale tornado regimes. Electron. J. Severe Storms Meteor., 8 (3), https://ejssm.org/ojs/index.php/ejssm/article/viewArticle/119.
- Geerts, B., and M. Noke-Raico, 1995: Tornadoes in Australia: Do we really know? Bull. Aust. Meteor. Oceanogr. Soc., 8, 46–51.
- Gelaro, R., and Coauthors, 2017: The Modern-Era Retrospective Analysis for Research and Applications, version 2 (MERRA-2). J. Climate, 30, 5419–5454, https://doi.org/10.1175/JCLI-D-16-0758.1.
- Gensini, V. A., and L. Bravo de Guenni, 2019: Environmental covariate representation of seasonal U.S. tornado frequency. J. Appl. Meteor. Climatol., 58, 1353–1367, https://doi.org/ 10.1175/JAMC-D-18-0305.1.
- Grams, J. S., R. L. Thompson, D. V. Snively, J. A. Prentice, G. M. Hodges, and L. J. Reames, 2012: A climatology and comparison of parameters for significant tornado events in the United States. Wea. Forecasting, 27, 106–123, https://doi.org/10.1175/WAF-D-11-00008.1.
- Grazulis, T. P., 1993: Significant Tornadoes 1680-1991: A Chronology and Analysis of Events. Environmental Films, 1340 pp.
- Hampshire, N. L., R. M. Mosier, T. M. Ryan, and D. E. Cavanaugh, 2018: Relationship of low-level instability and tornado damage rating based on observed soundings. *J. Operational Meteor.*, 6, 1–12, https://doi.org/10.15191/nwajom.2018.060.
- Hanstrum, B. N., G. A. Mills, A. Watson, J. P. Monteverdi, and C. A. Doswell III, 2002: The cool-season tornadoes of California and Southern Australia. *Wea. Forecasting*, 17, 705–722, https://doi.org/10.1175/1520-0434(2002)017<0705: TCSTOC>2.0.CO;2.
- Johns, R. H., J. M. Davies, and P. W. Leftwich, 1993: Some wind and instability parameters associated with strong and violent tornadoes: 2. Variations in the combinations of wind and instability parameters. *The Tornado: Its Structure, Dynamics, Prediction, and Hazards, Geophys. Monogr.*, Vol. 79, Amer. Geophys. Union, https://doi.org/10.1029/GM079p0583.
- Jones, T., P. Skinner, N. Yussouf, K. Knopfmeier, A. Reinhart, and D. Dowell, 2019: Forecasting high-impact weather in landfalling tropical cyclones using a Warn-on-Forecast system. *Bull. Amer. Meteor. Soc.*, 100, 1405–1417, https://doi.org/ 10.1175/BAMS-D-18-0203.1.
- Keul, A. G., and Coauthors, 2018: Multihazard weather risk perception and preparedness in eight countries. Wea. Climate Soc., 10, 501–520, https://doi.org/10.1175/WCAS-D-16-0064.1.
- King, J. R., M. D. Parker, K. D. Sherburn, and G. M. Lackmann, 2017: Rapid evolution of cool season, low-CAPE severe thunderstorm environments. Wea. Forecasting, 32, 763–779, https://doi.org/10.1175/WAF-D-16-0141.1.
- Knapp, K. R., M. C. Kruk, D. H. Levinson, H. J. Diamond, and C. J. Neumann, 2010: The International Best Track Archive for Climate Stewardship (IBTrACS) unifying tropical cyclone data. *Bull. Amer. Meteor. Soc.*, 91, 363–376, https://doi.org/ 10.1175/2009BAMS2755.1.
- Kounkou, R., G. Mills, and B. Timbal, 2009: A reanalysis climatology of cool-season tornado environments over southern

- Australia. *Int. J. Climatol.*, **29**, 2079–2090, https://doi.org/10.1002/joc.1856.
- Louis, S. A., 2018: A warm-front triggered nocturnal tornado outbreak near Kiama, NSW, Australia. J. Southern Hemisphere Earth Syst. Sci., 68, 147–164, https://doi.org/10.1071/ES18008.
- McCaul, E. W., Jr., 1991: Buoyancy and shear characteristics of hurricane–tornado environments. *Mon. Wea. Rev.*, **119**, 1954–1978, https://doi.org/10.1175/1520-0493(1991)119<1954: BASCOH>2.0.CO:2.
- Mills, G., and J. Colquhoun, 1998: Objective prediction of severe thunderstorm environments: Preliminary results linking a decision tree with an operational regional NWP model. *Wea. Forecasting*, **13**, 1078–1092, https://doi.org/10.1175/1520-0434(1998)013<1078:OPOSTE>2.0.CO:2.
- Mills, G. A., 2004: Verification of operational cool-season tornado threat-area forecasts from mesoscale NWP and a probabilistic forecast product. Aust. Meteor. Mag., 53, 269–277.
- Minor, J. E., R. E. Peterson, and R. Lourensz, 1980: Characteristics of Australian tornadoes. *Aust. Meteor. Mag.*, **28**, 57–77.
- Munro, C., 2011: Review of the Bureau of Meteorology's Capacity to Respond to Future Extreme Weather and Natural Disaster Events and to Provide Seasonal Forecasting Services. Department of Sustainability, Environment, Water, Population and Communities, 122 pp.
- Niino, H., T. Fujitani, and N. Watanabe, 1997: A statistical study of tornadoes and waterspouts in Japan from 1961 to 1993. *J. Climate*, **10**, 1730–1752, https://doi.org/10.1175/1520-0442(1997)010<1730:ASSOTA>2.0.CO;2.
- Onderlinde, M. J., and H. E. Fuelberg, 2014: A parameter for forecasting tornadoes associated with landfalling tropical cyclones. Wea. Forecasting, 29, 1238–1255, https://doi.org/10.1175/ WAF-D-13-00086.1.
- Peterson, C. J., 2007: Consistent influence of tree diameter and species on damage in nine eastern North America tornado blowdowns. For. Ecol. Manage., 250, 96–108, https://doi.org/ 10.1016/j.foreco.2007.03.013.
- Potvin, C. K., K. L. Elmore, and S. J. Weiss, 2010: Assessing the impacts of proximity sounding criteria on the climatology of significant tornado environments. *Wea. Forecasting*, **25**, 921–930, https://doi.org/10.1175/2010WAF2222368.1.
- Ramsay, H., J. T. Allen, and J. Hall, 2013: The Australia Day 2013 tornado outbreak in southeast Queensland associated with extropical cyclone Oswald. *Tenth Annual Meeting of the Asia Oceania Geosciences Society*, Brisbane, Australia, Asia Oceania Geosciences Society (AOGS).
- Rasmussen, E. N., 2003: Refined supercell and tornado forecast parameters. *Wea. Forecasting*, **18**, 530–535, https://doi.org/10.1175/1520-0434(2003)18<530:RSATFP>2.0.CO:2.
- Rauhala, J., and D. M. Schultz, 2009: Severe thunderstorm and tornado warnings in Europe. Atmos. Res., 93, 369–380, https:// doi.org/10.1016/j.atmosres.2008.09.026.
- Richter, H., 2007: A cool season low-topped supercell tornado event near Sydney, Australia. *33rd Conf. on Radar Meteorology*, Cairns, Australia, Amer. Meteor. Soc., https://ams.confex.com/ams/33Radar/webprogram/Paper123550.html.
- Sherburn, K. D., and M. D. Parker, 2014: Climatology and ingredients of significant severe convection in high-shear, low-CAPE environments. Wea. Forecasting, 29, 854–877, https://doi.org/10.1175/WAF-D-13-00041.1.
- —, —, J. R. King, and G. M. Lackmann, 2016: Composite environments of severe and nonsevere high-shear, low-CAPE convective events. *Wea. Forecasting*, 31, 1899–1927, https:// doi.org/10.1175/WAF-D-16-0086.1.

- Sills, D. M., J. W. Wilson, P. I. Joe, D. W. Burgess, R. M. Webb, and N. I. Fox, 2004: The 3 November tornadic event during Sydney 2000: Storm evolution and the role of low-level boundaries. *Wea. Forecasting*, 19, 22–42, https://doi.org/10.1175/1520-0434(2004) 019<0022:TNTEDS>2.0.CO;2.
- Soderholm, J. S., M. R. Kumjian, N. McCarthy, P. Maldonado, and M. Wang, 2020a: Quantifying hail size distributions from the sky: Application of drone aerial photogrammetry. *Atmos. Meas. Tech.*, 13, 747–754, https://doi.org/10.5194/ amt-13-747-2020.
- —, K. I. Turner, J. P. Brook, T. Wedd, and J. Callaghan, 2019: High-impact thunderstorms of the Brisbane metropolitan area. J. Southern Hemisphere Earth Syst. Sci., 69, 239–251, https://doi.org/10.1071/ES19017.
- Speer, M. S., P. Wiles, and A. Pepler, 2009: Low pressure systems off the New South Wales coast and associated hazardous weather: Establishment of a database. *Aust. Meteor. Oceanogr. J.*, 58, 29–39, https://doi.org/10.22499/ 2.5801.004.
- SREP, 2015: Bureau of Meteorology Strategic Radar Enhancement Project. Australian Bureau of Meteorology, accessed 25 November 2015, http://www.bom.gov.au/australia/radar/about/srep.shtml.
- Stull, R., 2000: *Meteorology for Scientists and Engineers*. Brooks/Cole, 502 pp.
- Taszarek, M., and L. Kolendowicz, 2013: Sounding-derived parameters associated with tornado occurrence in Poland and

- universal tornadic index. *Atmos. Res.*, **134**, 186–197, https://doi.org/10.1016/j.atmosres.2013.07.016.
- —, J. Allen, T. Púčik, K. Hoogewind, and H. Brooks, 2020: Severe convective storms across Europe and the United States. Part II: Environments accompanying lightning, large hail, severe wind and tornadoes. J. Climate, 33, 10 263–10 286, https://doi.org/10.1175/JCLI-D-20-0346.1.
- The New Daily, 2015: Tornado warning issued for sydney. *The New Daily*, accessed 11 February 2020, https://thenewdaily.com.au/news/state/nsw/2015/12/16/tornado-warning-issued-sydney/.
- The Weather Chaser, 2017: Australian Weather Radar Archive. Bureau of Meteorology Historical Radar Data, The Weather Chaser, accessed 14 July 2017, http://www.theweatherchaser.com/radar-loop/.
- Thompson, R. L., R. Edwards, J. A. Hart, K. L. Elmore, and P. Markowski, 2003: Close proximity soundings within supercell environments obtained from the Rapid Update Cycle. *Wea. Forecasting*, **18**, 1243–1261, https://doi.org/10.1175/1520-0434(2003)018<1243:CPSWSE>2.0.CO;2.
- Tippett, M. K., C. Lepore, and J. E. Cohen, 2016: More tornadoes in the most extreme U.S. tornado outbreaks. *Science*, **354**, 1419–1423, https://doi.org/10.1126/science.aah7393.
- Verbout, S. M., D. M. Schultz, L. M. Leslie, H. E. Brooks, D. Karoly, and K. L. Elmore, 2007: Tornado outbreaks associated with landfalling hurricanes in the North Atlantic basin: 1954–2004. *Meteor. Atmos. Phys.*, 97, 255–271, https://doi.org/ 10.1007/s00703-006-0256-x.